Effects of Dopaminergic Modulation on the Integrative Properties of the Ventral Striatal Medium Spiny Neuron

Article *in* Journal of Neurophysiology · January 2008

DOI: 10.1152/jn.00335.2007 · Source: PubMed

3 authors, including:

Jason T Moyer
University of Pennsylvania
14 PUBLICATIONS **511** CITATIONS

SEE PROFILE

John Wolf
University of Pennsylvania
91 PUBLICATIONS **3,217** CITATIONS

SEE PROFILE

J Neurophysiol 98: 3731–3748, 2007.
First published October 3, 2007; doi:10.1152/jn.00335.2007.

Effects of Dopaminergic Modulation on the Integrative Properties of the Ventral Striatal Medium Spiny Neuron

Jason T. Moyer,[1] John A. Wolf,[2] and Leif H. Finkel[1]
[1]*Department of Bioengineering and* [2]*Department of Psychiatry, University of Pennsylvania, Philadelphia, Pennsylvania*

Submitted 26 March 2007; accepted in final form 3 October 2007

Moyer JT, Wolf JA, Finkel LH. Effects of dopaminergic modulation on the integrative properties of the ventral striatal medium spiny neuron. *J Neurophysiol* 98: 3731–3748, 2007. First published October 3, 2007; doi:10.1152/jn.00335.2007. Dopaminergic modulation produces a variety of functional changes in the principal cell of the striatum, the medium spiny neuron (MSN). Using a 189-compartment computational model of a ventral striatal MSN, we simulated whole cell D1- and D2-receptor–mediated modulation of both intrinsic (sodium, calcium, and potassium) and synaptic currents (AMPA and NMDA). Dopamine (DA) modulations in the model were based on a review of published experiments in both ventral and dorsal striatum. To objectively assess the net effects of DA modulation, we combined reported individual channel modulations into either D1- or D2-receptor modulation conditions and studied them separately. Contrary to previous suggestions, we found that D1 modulation had no effect on MSN nonlinearity and could not induce bistability. In agreement with previous suggestions, we found that dopaminergic modulation leads to changes in input filtering and neuronal excitability. Importantly, the changes in neuronal excitability agree with the classical model of basal ganglia function. We also found that DA modulation can alter the integration time window of the MSN. Interestingly, the effects of DA modulation of synaptic properties opposed the effects of DA modulation of intrinsic properties, with the synaptic modulations generally dominating the net effect. We interpret this lack of synergy to suggest that the regulation of whole cell integrative properties is not the primary functional purpose of DA. We suggest that D1 modulation might instead primarily regulate calcium influx to dendritic spines through NMDA and L-type calcium channels, by both direct and indirect mechanisms.

INTRODUCTION

Dysfunction in the dopamine (DA) modulatory system is involved in a number of clinical disorders, including Parkinson's disease, drug addiction, and schizophrenia. One of the major sites of dopaminergic innervation in the brain is the striatum, consisting of the dorsal striatum (which includes the caudate and putamen) and the ventral striatum (which includes the nucleus accumbens core and shell). The principal cell of the striatum is the medium spiny projection neuron (MSN), which constitutes between 85 and 95% of the total cell population, depending on the species and relative location in the striatum (O'Donnell and Grace 1993; Tepper et al. 2004).

The effects of DA on the MSN have been extensively studied and depend on the class of receptor expressed by the cell. Most MSNs coexpress two or more species of receptors, although D1 and D2 receptors (D1R and D2R, respectively) are the most prevalent. D2, D3, and D4 receptors are pharmacologically similar, as are D1 and D5 receptors (Vallone et al. 2000). Research to date suggests that striatal MSNs express primarily either D1Rs or D2Rs (Gerfen et al. 1990; Le Moine and Bloch 1996; Maurice et al. 1999; Surmeier et al. 1996; Yung et al. 1995). The specific effects of D3-, D4-, and D5-receptor activation on MSN channels have not been extensively investigated.

DA modulates several intrinsic and synaptic channels of MSNs, including sodium, potassium, and calcium species, as well as α-amino-3-hydroxy-5-methyl-4-isoxazolepropionic acid (AMPA) and *N*-methyl-D-aspartate (NMDA) receptors (Nicola et al. 2000). Generally, the direction of modulation (increase or decrease of conductance) for each channel is dependent on the type of DA receptor stimulated. Presumably, the effect of DA modulation on MSN function is the result of a combination of several individual intrinsic and synaptic channel modulations. However, most studies that sought to examine the effects of net DA modulation have failed to generate consistently reproducible, widely accepted results, whereas several other studies have led to the development of hypotheses that are difficult to examine experimentally.

Using a 189-compartment computational model of the nucleus accumbens core MSN (Wolf et al. 2005b), we investigate three previously proposed effects of dopaminergic modulation on the integrative properties of striatal MSNs, as well as one novel hypothesis. The first effect we investigated is the hypothesis that D1R-mediated modulation increases the nonlinearity of MSN cell output in response to synaptic input (Gruber et al. 2003; Hernández-López et al. 1997; Nicola et al. 2000). This hypothesis is based on the observation that MSN cells in in vivo anesthetized preparations oscillate between a hyperpolarized membrane potential (down-state) and a depolarized plateau potential in which the cell may generate action potentials (up-state) (Goto and O'Donnell 2001; Stern et al. 1997; Tseng et al. 2001; Wickens and Wilson 1998; Wilson and Kawaguchi 1996). In this context, DA-enhanced nonlinearity would increase the tendency for the cell to dwell in one of these two states, potentially contributing to gating (O'Donnell and Grace 1995), pattern recognition (Houk 1995), or credit assignment (Kerr and Plenz 2002, 2004) at the network level. The second proposed effect is that DA activation of D1Rs increases striatal output, whereas D2R activation reduces striatal output (Albin et al. 1989; Bamford et al. 2004; Cepeda and Levine 1998; Delong 1990; Gonon 1997; Goto and Grace 2005b). This hypothesis underlies an influential model of basal ganglia function, in which DA regulates the balance of the

Address for reprint requests and other correspondence: J. T. Moyer, Dept. of Bioengineering, 210 S. 33rd St., 240 Skirkanich Hall, Philadelphia, PA 19104 (E-mail: jtmoyer@seas.upenn.edu).

The costs of publication of this article were defrayed in part by the payment of page charges. The article must therefore be hereby marked "*advertisement*" in accordance with 18 U.S.C. Section 1734 solely to indicate this fact.

direct, D1R-expressing, movement-facilitatory pathway and the indirect, D2R-expressing, movement-inhibitory pathway (Albin et al. 1989; Delong 1990). In this model, loss of DA innervation to the striatum, as in Parkinson's disease, biases control of the basal ganglia output toward the movement-inhibiting indirect pathway, resulting in deficits in movement initiation and execution. The third previously proposed effect hypothesizes that DA acts as an input filtering mechanism, suppressing weak inputs while permitting or even enhancing stronger inputs (Cepeda and Levine 1998; Hjelmstad 2004; Nicola et al. 2000, 2004). This could enhance the signal-to-noise ratio of MSN inputs. We also investigated a novel hypothesis, that dopamine might affect the integration time window of the MSN. In this scenario, dopamine could alter the integrative behavior of striatal cells, shifting their behavior in the direction of either integration or coincidence detection. Such an effect could presumably modulate the overall integration of inputs in the corticostriatal network, which may affect the behavioral output of the system.

We found that dopaminergic modulation had no effect on nonlinearity or bistability of the MSN, except at very high, apparently nonphysiological levels of NMDA conductance. DA modulation was able to regulate neuronal excitability and input filtering in the MSN and was also capable of modulating the temporal integrative properties of the MSN. In these cases, the synaptic effects of DA modulation counteracted and overcame the intrinsic effects of DA modulation.

METHODS

The model was developed in the NEURON simulation environment (Carnevale and Hines 2005; Hines and Carnevale 1997). Simulations were performed on a dual 2.5-GHz Power Macintosh G5 (Apple Computers, Cupertino, CA) or in parallel on a 12-node cluster with dual 2.8-GHz processors per node (Penguin Computing, San Francisco, CA). Data analysis was performed using MATLAB (The MathWorks, Natick, MA).

Morphology and physiology of the model

The MSN model has been previously described in detail (Wolf et al. 2005b), so we focus on the most salient aspects of the model in this section. Specifics of the model, including channel parameters and cell morphology, are described in more detail in the supplementary material.[1] Cell dimensions (dendritic length and diameter, soma size) and passive properties were set to match published values (O'Donnell and Grace 1993; Wilson 1992). The model consists of 189 compartments and includes almost all intrinsic currents known to be expressed in the MSN, including: fast (NaF) and persistent sodium (NaP); fast-inactivating (KAf) and slow-inactivating (KAs) A-type, 4-aminopyridine (4-AP)–resistant, persistent delayed-rectifying (KRP), and inward-rectifying (KIR) potassium currents; large-conductance (BK) and small-conductance (SK) calcium-dependent potassium currents; N- (CaN), P/Q- (CaP/Q), R- (CaR), and L-type (Cav1.2) high-voltage–activated calcium channels; and T- (CaT) and L-type (Cav1.3) low-voltage–activated calcium channels. These channels were distributed throughout the cell in accordance with published data when possible. If not known, channels were assumed to be distributed uniformly throughout the cell unless this resulted in nonphysiological behavior (see Wolf et al. 2005b). All biophysical and kinetic properties for each channel in the model were taken directly from published data (Wolf et al. 2005b). Channel kinetics and voltage dependencies from channels isolated in striatal MSN cells were used when available. Spines were not explicitly modeled, but we accounted for their contribution to membrane area (Segev and Burke 1998). Each tertiary dendrite consisted of 11 compartments to ensure spatial accuracy, and inputs were placed in the middle of the appropriate compartment to acquire second-order correct solutions (Carnevale and Hines 2005).

The internal calcium concentration in a thin shell just inside the cell membrane was tracked for each compartment. BK and SK currents were regulated by calcium influx by N-, P/Q-, and R-type calcium channels, whereas the remaining calcium currents contributed to a separate pool based on published experimental results (Vilchis et al. 2000).

High-calcium retuning of the model

The model was tuned by hand to in vitro data, changing only the conductance and subcellular localization of each of the channels (except for NaF activation/inactivation), which involved an extensive exploration of the parameter space and the selection of the tunings that best fit in vitro data. Because the level of calcium expression in MSN cells can vary significantly (Bargas et al. 1994; Churchill and Macvicar 1998; Hoehn et al. 1993), and DA has been shown to modulate several calcium channels, we created a new version of the model with approximately tenfold higher calcium channel expression than that of the "low-calcium" version presented previously (Wolf et al. 2005b; see Table 1 for comparison). We ran all experiments with both tunings to more fully explore the range of effects of DA on MSNs. The results of experiments on the high-calcium tuning are presented in the main figures and the results using the previous, low-calcium tuning (Wolf et al. 2005b) are included in the supplemental material (Supplementary Figs. 2–5) for reference.

The high-calcium tuning was modified in four ways from the previous, low-calcium tuning (Wolf et al. 2005b). First, calcium channel expression was increased to support calcium spiking. Second, SK current expression was changed from uniform expression throughout the cell to expression in the secondary and tertiary dendrites only, in agreement with studies suggesting that SK channels are expressed primarily in dendritic spines (Faber et al. 2005; Ngo-Anh et al. 2005; Obermair et al. 2003). Third, a rapidly activating, delayed rectifier Kv1.3 (KDR) current was added at uniform conductance throughout the cell. Fourth, the cell was retuned after these changes to match in vitro current-clamp data, including spike shape, frequency response, and subthreshold membrane response of a nucleus accumbens core cell (see RESULTS). This included changing the maximum conductance of many channels and implementing a −2-mV shift of the fast sodium channel (Table 1).

Calcium channel density in the cell was increased for all classes of calcium in comparison to the low-calcium version (Wolf et al. 2005b) (see Table 1). Our previous model was based on studies of acutely dissociated cells (Churchill and Macvicar 1998) and represented an estimate of whole cell calcium current levels. The fact that cellular expression of calcium channels may be largely dendritic (Carter and Sabatini 2004; Day et al. 2006; Kerr and Plenz 2002; Olson et al. 2005) suggests that our previous estimate may represent a cell with relatively low levels of calcium expression. Further, at least some striatal cells exhibit calcium spiking after 4-aminopyridine (4-AP) and tetrodotoxin (TTX) application (O'Donnell and Grace 1993), which was not supported in the previous model. Because cells exhibiting calcium spikes presumably represent cells with relatively high levels of calcium expression, we increased calcium expression approximately tenfold and retuned the rest of the model's parameters to support calcium spiking to verify the robustness of our results. Future experimental work will be necessary to provide a more accurate determination of the range of expression of calcium currents in the adult striatal neuron.

D1 modulation decreases the SK current (by CaN and CaQ reduction) and increases the Cav1.3 calcium current; both of these modu-

[1] The online version of this article contains supplemental data.

TABLE 1. *Channel parameters and changes in cell tuning*

	Gbar, S/cm^2	HH Form	V_{half}, mV	Slope, mV	Change From Previous
NaF	1.875, soma	$m^3 \times h$	m − 25.9	−11.8	×1.25
	0.0244, dends		h − 64.9	10.7	m and h shifted −2 mV
NaP	5×10^{-5}, soma	m × h	m − 52.6	−4.6	×1.25
	1.73×10^{-7}, dends		h − 48.8	10.0	
KAf	0.36, soma and prox	$m^2 \times h$	m − 10.0	−17.7	×1.6
	0.033, mid and dist		h − 75.6	10.0	
KAs	0.0104, soma and prox	$m^2 \times [ah + (1 - a)]$	m − 27.0	−16.0	No change
	9.51×10^{-4}, mid and dist	a = 0.996	h − 33.5	21.5	
KIR	1.4×10^{-4}	m	m − 52.0	17.5	No change
			mshift = 25		
KRP	1.5×10^{-4}, soma and prox	m × [ah + (1 − a)]	m − 13.5	−11.8	×0.15
		a = 0.7	h − 54.7	18.6	
KDR	0.0005	m^4	See *Eqs.* A*3* and A*4*		New channel
BK Kca	0.12				×120
SK Kca	0.1885, mid and dist				×1.3; mid and dist only
Leak	11.5×10^{-6}				No change
	Pbar, cm/s	HH Form	V_{half}, mV	Slope, mV	Change From Previous
$Ca_v1.2$	6.7×10^{-5}	$m^2 \times [ah + (1 - a)]$	m − 8.9	−6.7	×10
		a = 0.17	h − 13.4	11.9	
$Ca_v1.3$	3.19×10^{-5}, soma and prox	$m^2 \times h$	m − 33.0	−6.7	×75, soma and prox
	4.25×10^{-6}, mid and dist		h − 13.4	11.9	×10, mid and dist
CaN	1.0×10^{-4}	$m^2 \times [ah + (1 - a)]$	m − 8.7	−7.4	×10
		a = 0.21	h − 74.8	6.5	
CaP/Q	6.0×10^{-5}	m^2	m − 9.0	−6.6	×10
CaR	2.6×10^{-4}	$m^3 \times h$	m − 10.3	−6.6	×10
			h − 33.3	17.0	
CaT	4.0×10^{-6}	$m^3 \times h$	m − 51.73	−6.53	×10
			h − 80.0	6.7	

Changes in cell tuning (listed as multiples) are compared to a previous, low-calcium tuning of the model (Wolf et al. 2005).

lations can enhance the tendency of the model to spike in doublets. To our knowledge, D1 modulation has not been observed to induce doublets, but at the extreme modulation levels that we study here we occasionally observed doublets at high-input levels. To address this, we added a Kv1.3, fast-activating delayed-rectifier potassium current (KDR) throughout the cell (Erisir et al. 1999). It is similar to the KRP current (Nisenbaum et al. 1996) in that it is a tetraethylammonium (TEA)-sensitive, delayed-rectifier current. However, it activates about fivefold faster and at more hyperpolarized potentials, allowing it to suppress doublets without significantly affecting subthreshold activity. We used the Kv1.3 because it has been well characterized in a computational model (Erisir et al. 1999) and behaves similarly to the Kv1.1 and Kv1.6 channels (Coetzee et al. 1999), which have been detected in MSN cells using mRNA assays (Shen et al. 2004). Accordingly, we implemented the Kv1.3 channel as a substitute for the Kv1.1/1.6 channels and suggest that these currents may represent a portion of the TEA-sensitive, delayed-rectifier current in MSNs. The KDR channel was inserted at a uniform conductance of 5.0×10^{-4} S/cm^2 throughout the cell.

Dopaminergic modulation

Dopamine has been reported to modulate a number of channels in MSNs. We performed a thorough review of the literature on dopaminergic modulation in both dorsal and ventral striatum, by both D1 and D2 receptors (Table 2). Although historically theories regarding the net effects of dopaminergic modulation on MSNs have been conflicting (Nicola et al. 2000), most studies on DA modulation of individual channels agree on both the direction and magnitude of modulation. The dopaminergic modulation conditions we used for our study are listed in Table 3; these modulations are drawn entirely from the studies listed in the literature review in Table 2. Values in Table 3 are listed as percentage changes of the baseline maximum conductance or as voltage shifts (in millivolts) for the appropriate channel parameter. An in-depth discussion of the rationale behind the modulations we used is provided in the APPENDIX.

To be as objective as possible, we created modulation conditions (Table 3) that accounted for all channel modulations reported in the literature (most of which, as mentioned, do not contradict each other; see Table 2). It is possible that DA does not modulate all of these channels simultaneously in the same cell, as it does in our analysis. However, it is quite difficult to verify whether this is the case experimentally and, to our knowledge, no such study has ever been performed. Accordingly, because our goal is to fairly assess the net effects of DA on MSN function, we account for all reported D1R- and D2R-channel modulations in our study. Our results are not crucially sensitive to variations in modulation of a single channel, except when noted in the RESULTS.

We created four modulation conditions—D1 Intrinsic, D1 All, D2 Intrinsic, and D2 All—based entirely on published results (Table 3). The D1 and D2 Intrinsic conditions consisted solely of intrinsic channel (Na, K, Ca) modulations. The D1 and D2 All conditions consisted of the appropriate intrinsic modulation condition with synaptic (AMPA, NMDA) modulations included. These same modulation conditions were used for all experiments and applied uniformly to the entire cell. We studied D1 and D2 modulations in isolation, but did not investigate the condition in which these receptors may be coexpressed on the same cell.

For the nonlinearity study (Fig. 2) we investigated the possibility that very high levels of NMDA could induce bistability. We created a modulation condition (labeled "Nonphysiological") that included an NMDA conductance of 500% of the baseline, KAf 155% of the baseline, and KIR 350% of the baseline; the increases in KAf and KIR currents

TABLE 2. *Summary of studies on dopaminergic modulation of MSN channels*

	Dorsal Striatum		Ventral Striatum		
		A. D1			
NaF	D1: NaF ↓ 22–37.8% D1: NaF hV1/2 ← −5.6 mV	(Calabresi et al. 1987; Schiffmann et al. 1995, 1998; Surmeier et al. 1992)	NaF	D1: NaF ↓ 25%	(Zhang et al. 1998)
CaP/Q	D1: P/Q ↓ 16–83% (calc.)	(Salgado et al. 2005; Surmeier et al. 1995)	CaP/Q	D1: P/Q ↓ 48% (calc.)	(Zhang et al. 2002)
CaN	D1: N ↓ 4–23.5% (calc.)	(Salgado et al. 2005; Surmeier et al. 1995)	CaN	D1: N ↓ 80% (calc.)	(Zhang et al. 2002)
Cal.	D1: L ↑ 100% (est.)	(Nicola et al. 2000; Song and Surmeier 1996; Surmeier et al. 1995)	CaL	Unknown	
	D1: Lm (h?) V1/2 ←	(Surmeier et al. 1995)			
KAs	D1: KAs ↓ 5–20% D1: KAs no change	(Surmeier and Kitai 1993) (Hopf et al. 2003; Nisenbaum et al. 1998)	KAs	No change	(Hopf et al. 2003)
KIR	D1: KIR ↑ 25% (modeled)	(Pacheco-Cano et al. 1996)	KIR	D1: KIR ↑ 7%	(Uchimura and North 1990; Uchimura et al. 1986)
NMDA	D1: NMDA ↑ 3–41%	(Cepeda et al. 1998; Flores-Hemández et al. 2002; Hallett et al. 2006; Levine et al. 1996)	NMDA	D1: NMDA ↑ 71%	(Harvey and Lacey 1997)
	D1: NMDA ↓ 19–30%	(Castro et al. 1999; Lin et al. 2003)			
AMPA	D1: AMPA ↑ 21–29%	(Price et al. 1999; Umemiya and Raymond 1997)	AMPA	D1: AMPA ↓ 36–56%	(Harvey and Lacey 1996)
	D1: AMPA ↔	(Levine et al. 1996)			
		B. D2			
NaF	D2: NaF ↑ 19%, hV1/2 → 3.2 mV	(Surmeier et al. 1992)	NaF	D2: NaF ↔	(White et al. 1997; Zhang et al. 1998)
	D2: NaF ↔, hV1/2 ← −16.9 mV			D2: NaF ↑ 25%	(Hu et al. 2005)
CaL	D2: 1.3 ↓ 19–24%	(Hernández-López et al. 2000; Olson et al. 2005; Salgado et al. 2005)	CaL	D2: L ↓	(Perez et al. 2005)
	1.2 unaffected	(Olson 2005)			
KAs	D2: KAs ↑ 4–8%	(Kitai and Surmeier 1993; Surmeier and Kitai 1993)	KAs	D2: KAs ↑	(Perez et al. 2006)
KIR	Unknown		KIR	D2: KIR ↓ 2–15%	(Perez et al. 2006; Uchimura and North 1990; Uchimura et al. 1986)
NMDA	D2: NMDA ↔	(Cepeda et al. 1998; Flores-Hernández et al. 2002; Levine et al. 1996; Lin et al. 2003)	NMDA	Unknown	
AMPA	D2: AMPA ↓ 15–28%	(Hernández-Echeagaray et al. 2004; (Levine et al. 1996)	AMPA	Unknown	
Glu	D2: Glu ↓ 5–100%	(Bamford et al. 2004; Hsu et al. 1995)	Glu	D2: Glu ↓ 8–60%	(O'Donnell and Grace 1994; Yim and Mogenson 1988)

Values are percentage changes in the maximum conductance of the appropriate channel or shifts in the activation/inactivation parameters (see supplemental material).

were needed to maintain the spike threshold of this condition near that of the unmodulated model.

Synaptic input generation

Explicit glutamatergic and GABAergic synapses were modeled using a modified two-state synapse with time constants set to published values (Chapman et al. 2003; Galarreta and Hestrin 1997; Gotz et al. 1997). Each glutamatergic synapse consisted of an AMPA and NMDA pair receiving the same input train. Glutamatergic synapses were placed throughout the dendrites, in accordance with published results (Gracy et al. 1999; Wilson 1992). GABAergic synapses were distributed throughout the cell but clustered near the soma in agreement with physiological data (Fujiyama et al. 2000; Pickel and Heras 1996). AMPA and NMDA channels contributed to the calcium pool not associated with the SK/BK currents: 10% of NMDA current and 0.5% of AMPA current were designated as calcium currents as described in previous studies (Burnashev et al. 1995). AMPA (Myme et al. 2003), NMDA (Dalby and Mody 2003), and γ-aminobutyric acid (GABA) (Nusser et al. 1998) conductance levels were set to published values.

Synaptic inputs were modeled using a modified version of the NetStim object provided in the NEURON package. Each synapse (AMPA/NMDA or GABA) received an independent spike train generated using MATLAB. Each spike train was generated using the following algorithm: first, a constant interspike interval (ISI) train was generated at the desired frequency. Each spike was then pulled anew from a Gaussian distribution centered at the original spike time. The resulting train was then randomly shifted; this process was repeated for each of the 168 total synapses. Input was generated by using a large shift (one ISI) and a large SD (1/4 of the ISI). In our experience, MSNs rarely spike at more than 10 Hz, which corresponds to a maximum physiological input frequency of 1,350 Hz (see RESULTS). Accordingly we did not investigate synaptic input at higher frequen-

TABLE 3. *Dopaminergic modulation conditions for MSN model*

A. D1

	D1 Intrinsic	D1 All
NaF	95%	95%
h shift	0 mV	0 mV
CaP/Q	50%	50%
CaN	20%	20%
$Ca_v1.3$	100%	100%
m shift	−10 mV	−10 mV
$Ca_v1.2$	200%	200%
KAs	No change	No change
KIR	125%	125%
NMDA	100%	**130%**
AMPA	100%	**100%**

B. D2

	D2 Intrinsic	D2 All
NaF	110%	110%
h shift	3 mV	3 mV
Ca_v 1.3	75%	75%
m shift	0 mV	0 mV
Ca_v 1.2	100%	100%
KAs	110%	110%
KIR	100%	100%
NMDA	100%	**100%**
AMPA	100%	**80%**

Values are percentages of the unmodulated conductance; i.e., 100% indicates no modulation.

cies. The ratio of glutamatergic inputs to GABA inputs was held constant at roughly 1:1 for all simulations (Blackwell et al. 2003).

Simulations

Calcium spiking was examined by simulating the application of 50 μM 4-AP and 2 μM TTX during a current injection of 0.6 nA (O'Donnell and Grace 1993). To do this, we multiplied the KAf conductance by 0.9 (Song et al. 1998), KAs by 0.4 (Russell et al. 1994), KRP by 0.8 (Nisenbaum et al. 1996), and KDR by 0.6 (Coetzee et al. 1999). The NaF conductance was adjusted to match in vitro behavior, which required multiplying the baseline conductance by 0.25 (Fig. 1*B*).

Nonlinearity/bistability of the model's response to synaptic input (Fig. 2, *A–C*) was studied by holding the cell at a down-state input frequency (350 Hz) for 200 ms and then stepping it to evenly spaced frequencies between 350 and 1,100 Hz and holding for 500 ms. We also calculated spike frequency (Fig. 3*B*) from these data. Hysteresis in the model was examined by holding the model at a down-state input frequency (350 Hz) for 300 ms, increasing synaptic input smoothly to 850 Hz over 50 ms, holding it there for 600 ms, and then ramping input frequency back down at the same rate. We reflected the averaged (40 trials) cell voltage versus time on the down-slope of the ramp and plotted it against the averaged cell voltage versus time on the up-slope of the ramp for the unmodulated and D1 All conditions (Fig. 2*D*).

We examined the effects of DA modulation on the model's filtering of synaptic inputs of varying strengths and locations (Fig. 4). These simulations were performed while the model was receiving synaptic input at a frequency of 1,050 Hz. Synaptic input size was changed by multiplying the maximum conductance of the appropriate glutamatergic input by weights between 0.2 and 2.2. A weight of 1.0 corresponds to previously published values for conductance (Dalby and Mody 2003; Myme et al. 2003; Nusser et al. 1998).

We examined the integration time window of the model (Figs. 5, *A* and *B*) using a sliding-window analysis of the inputs to the cell while receiving subthreshold synaptic input. The size of the window was varied between 20 and 120 ms. At each time step, the inputs in the preceding, appropriately sized time window were counted and the corresponding instantaneous input frequency was calculated. This calculation was performed over a 13-s-long experiment in which the cell received synaptic input at 800 Hz—enough to hold it near −60 mV but not spike. The somatic voltage and the input frequency were normalized to a minimum of zero and a maximum of 1, and then the zeroth-lag correlation coefficient between the two was calculated using the corrcoef function in MATLAB.

We also calculated the probability that the cell would spike in response to synaptic stimulation of different intensities and different coherences. While the model was receiving synaptic input at a frequency of 800 Hz, we stimulated a given number of glutamatergic synapses, randomly distributed throughout the cell, every 200 ms (Fig. 5*C*). The number of spikes occurring within 40 ms after stimulation were divided by the number of stimulations during a 13-s simulation to calculate the probability of spiking. A second experiment examined how coherent these inputs needed to be to elicit a spike (Fig. 5*D*). In this experiment, while the model was receiving 800-Hz input, we

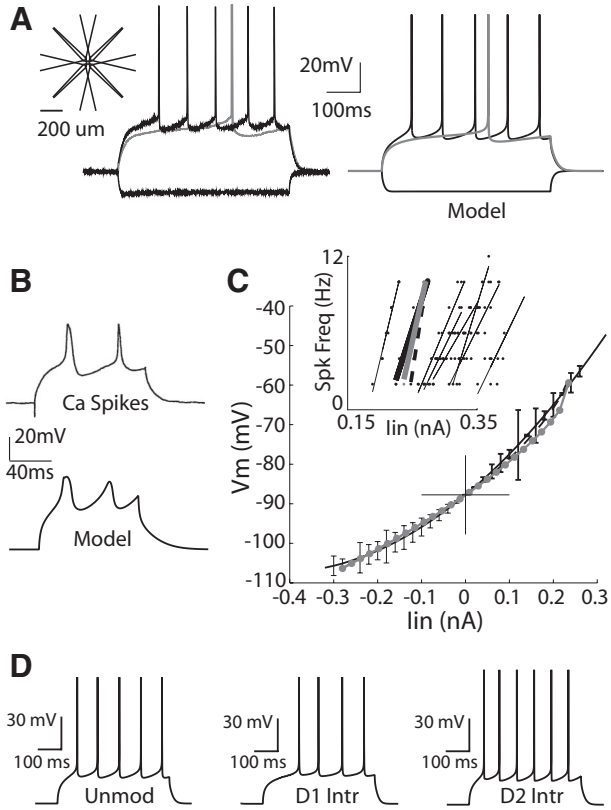

FIG. 1. Behavior of the model. *A*: model morphology (*inset*), in vitro response of a nucleus accumbens core medium spiny neuron (MSN) to current injections of −0.227, 0.225, and 0.271 nA (*left*), and the model's response to current injections of −0.227, 0.2375, and 0.271 nA (*right*). Model was retuned from a previous version (Wolf et al. 2005b) to represent an MSN with higher levels of calcium expression and used for all figures in the present study. *B*: calcium spikes in neonatal MSN cells (*top*; from O'Donnell and Grace 1993) and the model (*bottom*) after tetrodotoxin (TTX) and 4-aminopyridine (4-AP) application. *C*: current–voltage (*I–V*) response of the model (gray), mean of 7 in vitro MSNs (solid black), and low-calcium model tuning (dashed black). Model's *I–V* response is within the SD (error bars) of the in vitro responses. *Inset*: spiking frequency vs. current (*F–I*) response of the model (gray), the representative MSN cell to which it was tuned (thick black), 6 other MSN cells (thin black), and low-calcium tuning (Wolf et al. 2005b) (dashed black line). *D*: model's response to 0.271-nA current injection in unmodulated state (*left*) and after D1-receptor (D1R)–mediated modulation (*middle*) and D2R-mediated modulation (*right*) of intrinsic channels. (Reprinted with permission of Wiley-Liss, Inc., a subsidiary of John Wiley & Sons, Inc.)

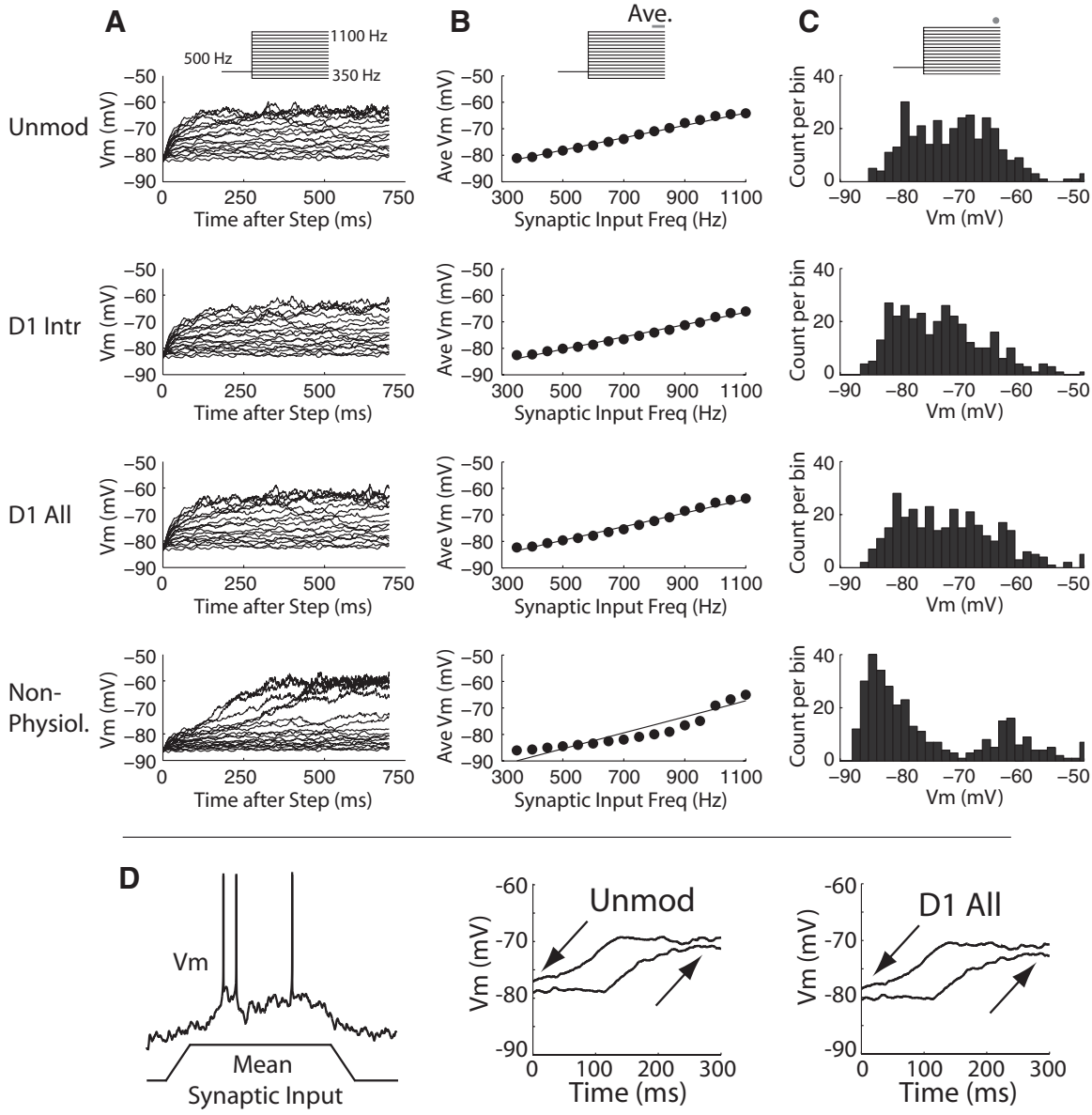

FIG. 2. Effects of D1R-mediated modulation on nonlinearity and hysteresis in the model. *A*: averaged response (18 trials) of the model to constant-frequency synaptic input in the unmodulated state (Unmod) and after D1R-mediated modulation of intrinsic channels (D1 Intr) and both intrinsic and synaptic channels (D1 All). In each trial, the model received synaptic input at 500 Hz for 200 ms, then the input was stepped to a new frequency and held for 700 ms (see *inset*). Input steps were linearly spaced between 350 and 1,100 Hz. *B*: averaged membrane potential (18 trials) vs. synaptic input frequency. Each point represents the average of the last 50 ms of the corresponding trace in Fig. 3A, with a least-squares linear fit drawn through the data for comparison. Neither the unmodulated, the D1 Intrinsic, nor the D1 All states exhibited nonlinearity. On dramatically increasing the *N*-methyl-D-aspartate (NMDA) conductance (500% of baseline), the model exhibited some nonlinearity (Non-Physiol), although this may be a nonphysiological level of NMDA (see DISCUSSION). *C*: membrane potential distribution in all trials 670 ms after the step in synaptic input frequency in the unmodulated (Unmod) condition and after D1R modulation of intrinsic channels only (D1 Intr) and D1R modulation of intrinsic and synaptic channels (D1 All). Distribution was unimodal in these conditions, but on dramatically increasing NMDA, the distribution became bimodal (Non-Physiol). *D*: hysteresis, or the difference between the V_m paths on the up- and down-slopes of a symmetric input ramp (*left*) does not change in the D1 All condition (*middle*) compared with the unmodulated condition (*right*). Taken together, these data suggest that in vivo MSNs are not inherently bistable and that D1 modulation does not contribute to nonlinearity in the MSN.

varied the width of the time window in which the synapses were activated. The exact times of the synaptic activations were random. Stimulation epochs were centered every 200 ms. We counted spikes that occurred during stimulation or within 40 ms following the center of the time window. The resulting spike count was divided by the number of stimulations to calculate the probability of spiking at each window width. For both experiments, the same synapses, randomly distributed throughout the cell, were activated for each stimulation. For the coincidence experiment (Fig. 5*D*), 15 synapses were stimulated for the unmodulated condition, 18 for the D1 Intrinsic, 14 for the D1 All, 13 for the D2 Intrinsic, and 18 for the D2 All; these numbers were used so that all conditions would have an approximately 90% chance of spiking in response to stimulation within a 2-ms window.

RESULTS

High-calcium version of the model

The model is a stylized representation of the nucleus accumbens core medium spiny neuron, with 189 compartments,

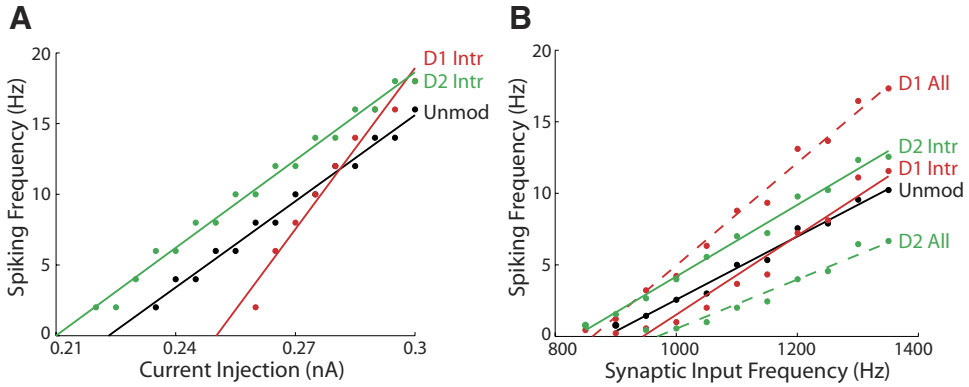

FIG. 3. Effects of D1R- and D2R-mediated modulation on model's excitability. *A*: spiking frequency vs. current injection for unmodulated (black), D1R-mediated (red: D1 Intrinsic), and D2R-mediated (solid green: D2 Intrinsic) modulation of intrinsic currents. D1R modulation increases the gain of the MSN from 203 (Unmod) to 380 Hz/nA (D1 Intrinsic). *B*: spiking frequency vs. synaptic input frequency for unmodulated (black: Unmod), D1R-mediated (solid red: D1 Intrinsic), and D2R-mediated (solid green: D2 Intrinsic) modulation of intrinsic properties. D1R modulation of both intrinsic and synaptic properties (D1 All) leads to excitation at all input levels (dashed red). D2R modulation of both intrinsic and synaptic properties (D2 All) leads to inhibition at all input levels (dashed green). D1R modulation increases the gain of the MSN model's response (Unmod = 0.0221 Hz/Hz, D1 Intrinsic = 0.0276 Hz/Hz, D1 All = 0.0359 Hz/Hz). Effects of synaptic modulations counteract the effects of intrinsic modulations on excitability in both the D1 All and D2 All conditions, and the resulting effects in these conditions agree with previous proposals regarding the effects of dopamine (DA) on MSN excitability.

branched dendrites, and explicit synapses (Fig. 1*A*, *inset*). The model was tuned to match the in vitro response to current injection of a nucleus accumbens core MSN isolated from an adult rat (Fig. 1*A*, *left*). Because the level of calcium expression in MSN cells can vary significantly (Bargas et al. 1994; Churchill and Macvicar 1998; Hoehn et al. 1993), and DA has been shown to modulate several calcium channels, we created a new tuning of the model with approximately tenfold higher calcium channel expression than that of the "low-calcium" version developed previously (Wolf et al. 2005b; see Table 1 for comparison). With this increased level of calcium, the model was able to approximate reports of calcium spiking in MSN cells after TTX and 4-AP application (Fig. 1*B*). We ran all experiments with both tunings to more fully explore the range of effects of DA on MSNs. We found that although the effects of DA on MSNs were generally more appreciable in the high-calcium tuning, the overall results of the experiments were the same. Results of experiments on the high-calcium tuning are presented in the main figures and results using the previous, low-calcium tuning are included in the supplemental material (Supplementary Figs. 2–5) for reference.

The high-calcium tuning of the model matched the frequency–current (*F–I*; gray line in Fig. 1*C*, *inset*) behavior of a representative in vitro MSN (Fig. 1*C*, *inset*, thick black line). This version of the model (Fig. 1*C*, gray trace) is also within the SD of the averaged current–voltage (*I–V*) response of seven MSNs (Fig. 1*C*, solid black trace). Interestingly, the high-calcium tuning (Fig. 1*C*, *inset*, gray trace) matches the *F–I* response of the representative cell better than the low-calcium version (Fig. 1*C*, *inset*, dashed black line), but has slightly more outward rectification (Fig. 1*C*, gray line) at depolarized potentials than the low-calcium version (Fig. 1*C*, dashed black line). This is primarily the result of redistribution of the SK current from uniform expression throughout the cell to only the secondary and tertiary dendrites.

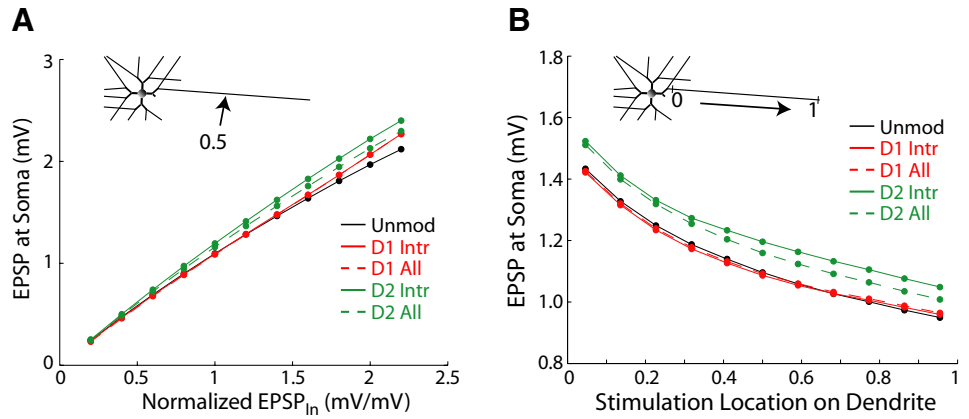

FIG. 4. Effects of D1R- and D2R-mediated modulation on MSN filtering of synaptic inputs. *A*: amplitude of glutamatergic excitatory postsynaptic potentials (EPSPs) measured at the soma as a function of size. Larger inputs are enhanced more than small inputs in the D1 Intrinsic (solid red), D1 All (dashed red), D2 Intrinsic (solid green), and D2 All (dashed green) modulation conditions compared with the unmodulated condition (black). *Inset*: arrow indicates stimulation site on MSN. *B*: amplitude of glutamatergic EPSPs as a function of position on tertiary dendrite. *Inset*: synaptic inputs of the same input amplitude were moved from the proximal tip to the distal tip of the tertiary dendrite. Neither D1 Intrinsic (solid red) nor D1 All (dashed red, between solid red and solid black lines) modulations significantly affect EPSP size at the soma compared with the unmodulated state (black). Both D2 Intrinsic (solid green) and D2 All (dashed green) modulation increase EPSP size at all positions. These findings agree with previous suggestions that DA modulation can preferably enhance the propagation of large synaptic inputs to the soma.

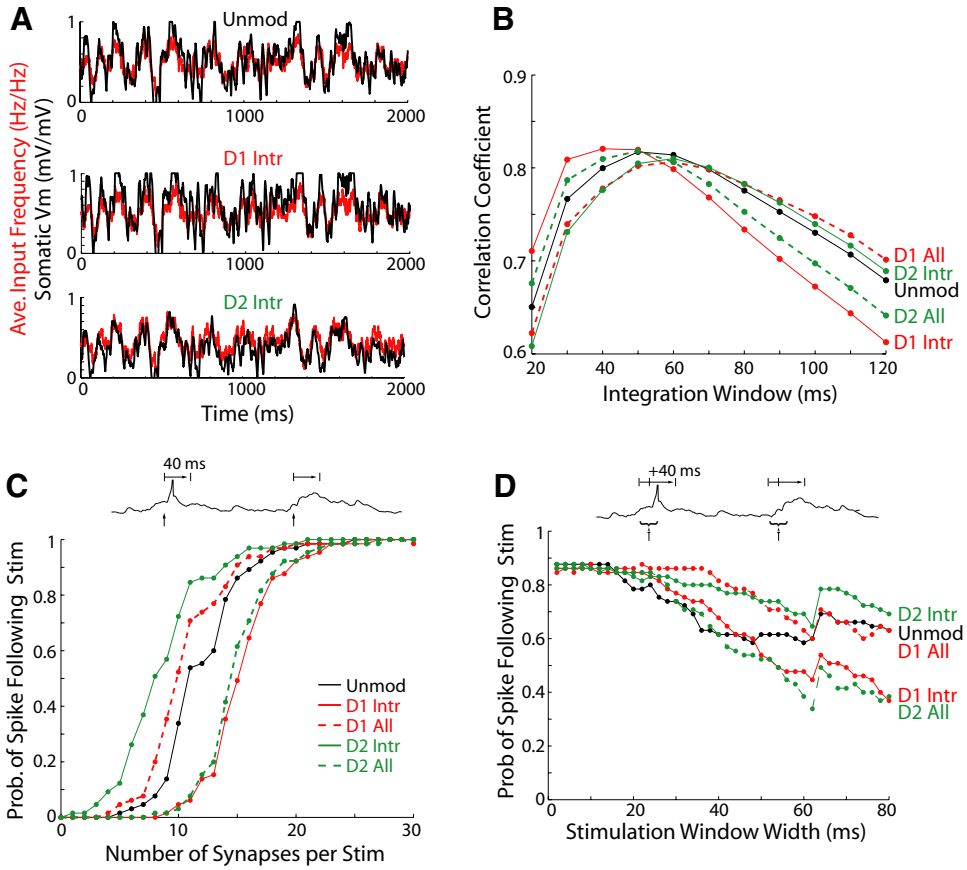

FIG. 5. Effects of D1R- and D2R-mediated modulation on MSN temporal integration of synaptic inputs. *A*: somatic V_m (black) and averaged input frequency using a sliding window of 50 ms (red) in the unmodulated (*top*) state and after D1 Intrinsic (*middle*) and D2 Intrinsic (*bottom*) modulation. *B*: zeroth-lag correlation of somatic V_m and averaged input frequency using different sliding window sizes. Unmodulated model correlates best with a window size of 50 ms (black). D1 Intrinsic modulation (solid red) decreases this window size to 40 ms, whereas D2 Intrinsic modulation (solid green) increases it to 60 ms. Including synaptic modulations reverses this effect, with D1 All (dashed red) modulation increasing the window to 60 ms and D2 All (dashed green) modulation decreasing it to 50 ms. Correlation was calculated over 13 s of subthreshold synaptic input (800 Hz). *C*: probability of the model spiking vs. number of synapses activated. Synapses were activated every 200 ms while the model was receiving subthreshold synaptic input at 800 Hz, and probability was calculated based on the number of spikes occurring within 40 ms of the stimulation (*inset*). With the same set of active synapses per stimulation, D1 Intrinsic (solid red) modulation makes the model less likely to spike, whereas D2 Intrinsic (solid green) makes the model more likely to spike. Including synaptic modulations reverses this relationship, with D1 All (dashed red) increasing the probability of spiking and D2 All (dashed green) decreasing it. *D*: probability of the model spiking vs. the width of the stimulation window. For each modulation condition, a set number of synapses were activated within a given time window, centered every 200 ms, and probability was calculated based on spikes occurring during the stimulation or ≤40 ms following the center of the stimulation window (*inset*). In general, D1 Intrinsic (solid red) modulation decreases the ability of the model to integrate synaptic inputs over larger time windows, whereas D2 Intrinsic (solid green) modulation increases its ability to do so relative to the unmodulated condition (black). Including synaptic modulations reverses this trend, with D1 All (dashed red) modulation generally improving the ability of the cell to integrate temporally dispersed input and D2 All (dashed green) modulation impairing this ability. These experiments suggest that DA modulation can alter the temporal integration window of the MSN.

Modulation conditions

Following a review of published D1R- and D2R-mediated modulations of MSN ionic channels (Table 2), we created four modulation conditions for use in this report (Table 3). These conditions represent the expected effects of solely D1 or solely D2 modulation of MSN channels (see METHODS). As much as possible, we used maximum reported levels of modulation because this should most clearly demonstrate the effects of D1R- and D2R-mediated modulation on MSN behavior. The D1 Intrinsic and D2 Intrinsic conditions include modulations of intrinsic channels only, whereas the D1 All and D2 All conditions account for synaptic modulations as well as intrinsic modulations (Table 3).

The D1 Intrinsic condition resulted in three primary changes: a delayed first spike, a relatively short interspike interval between the first and second spikes, and a reduced number of action potentials for a given current injection (Fig. 1*D*, *middle*). These observations agree with in vitro data (Hernández-López et al. 1997). The delay to first spike was primarily the result of increasing the KIR current. The relatively short interspike interval between the first and second spikes after the start of the current injection resulted primarily from the more hyperpolarized activation of the Cav1.3 current. The D2 Intrinsic condition resulted in deeper interspike troughs (Fig. 1*D*, *right*) and increased spiking, in agreement with previous observations in vitro (Akaike et al. 1987).

D1R-mediated modulation and nonlinearity in the MSN

It was previously proposed that D1R activation enhances nonlinearity in the MSN's response to synaptic input, perhaps even inducing bistable membrane behavior (see DISCUSSION for

our definitions of bistability, nonlinearity, and hysteresis) (Gruber et al. 2003; Hernández-López et al. 1997; Nicola et al. 2000). We examined this hypothesis in several ways. First, we examined the model's response to synaptic input applied at equally spaced increments from low to high frequency (Fig. 2*A*, *inset*). In this manner, we were able to examine whether the cell exhibited nonlinearity in response to the linear steps in input frequency (Fig. 2*A*; traces represent the average membrane potential for 18 trials). For clarity, we also plotted the average somatic potential of the model over the last 50 ms of each trace in Fig. 2*A* against the corresponding synaptic input frequency (Fig. 2*B*). Neither the unmodulated, D1 Intrinsic, or D1 All conditions exhibited any nonlinearity (Fig. 2, *A* and *B*). To see whether two distinct populations of membrane potential could be discerned across all 18 trials of 21 input frequencies, we created histograms of the membrane potential for each condition (Fig. 2*C*). Neither the unmodulated, D1 Intrinsic, nor the D1 All conditions appeared to express two appreciably distinct states for the membrane potential.

Following a recent study describing NMDA-dependent bistability in an MSN-like two-compartment computational model (Kepecs and Raghavachari 2007), we examined whether very high levels of NMDA might be able to induce nonlinearity or bistability (Fig. 2, *A–C*, *bottom*). We found that an NMDA:AMPA ratio >2.5:1 was required to induce two substantially distinct membrane potential states (Fig. 2*C*, *bottom*); this value appears to be outside the range of physiological ratios (see DISCUSSION; Myme et al. 2003). NMDA:AMPA ratios between 1:1 and 2.5:1 were not capable of inducing this behavior (data not shown).

We examined the response of the model for increased hysteresis after D1R modulation. To do this we ramped the frequency of synaptic input up and back down symmetrically (Fig. 2*D*, *left*) and averaged the membrane response across 40 trials of different inputs. Plotting the averaged cell voltage versus time on the down-slope of the ramp against the averaged cell voltage versus time on the up-slope of the ramp allows the paths to be compared (Fig. 2*D*). A bistable cell would have a highly asymmetric response to a symmetric input ramp, staying in the up-state even after removal of the input. The model MSN exhibits a small amount of asymmetry in the unmodulated condition, indicating that it is somewhat hysteretic in this condition (Fig. 2*D*, *middle*). D1 All modulation did not noticeably enhance this asymmetry (Fig. 2*D*, *right*). We previously showed that hysteresis in response to current injection is minimal compared with hysteresis in response to synaptic input (Wolf et al. 2005b); this is also the case for the D1-modulated cell in response to current injection (data not shown).

Taken together, these data suggest that D1 modulation does not enhance nonlinearity, except at potentially nonphysiological levels of NMDA. We found no evidence supporting MSN bistability under any modulation condition.

Excitatory/inhibitory properties of DA modulation

DA has long been hypothesized to be either excitatory or inhibitory based on the type of receptor activated. We focus on the hypothesis that D1R activation increases MSN activity, whereas D2R activation decreases MSN activity because these ideas underlie the most influential model of basal ganglia function to date (Albin et al. 1989; Delong 1990). Contrary to this idea, we found that the D2 Intrinsic condition increases spiking in response to current injection at all levels (Fig. 3*A*, solid green line) relative to the unmodulated condition (Fig. 3*A*, back line). Interestingly, the D1 Intrinsic condition is neither wholly excitatory nor inhibitory, but rather increases the slope of the *F–I* curve (Fig. 3*A*, red line). A change in gain response, and possible induction of nonlinearity, has been proposed as an important effect of D1 modulation on MSN function (Gruber et al. 2003; Hernández-López et al. 1997; Nicola et al. 2000). This has specifically been proposed to be the result of increases in KIR and Cav1.3 (Gruber et al. 2003). We found that KIR and Cav1.3 modulations contributed to the gain change, as did the CaP/Q and CaN modulations. The effects of D2 Intrinsic modulation are critically dependent on NaF modulation. As discussed in the APPENDIX, D2R activation may either increase or decrease sodium current (by conductance changes and inactivation curve shifts), depending on the recording method (Surmeier et al. 1992). We used a net increase in sodium (10% increase in conductance with a +3-mV shift of the inactivation curve) to agree with previous descriptions finding D2R activation to be mildly excitatory in response to current injection (Akaike et al. 1987; Higashi et al. 1989; Yim and Mogenson 1988). However, decreasing the net sodium current can substantially decrease spiking (not shown). Accordingly, the net effect of D2 Intrinsic modulation can be either excitatory or inhibitory, depending on the magnitude and direction of sodium modulation.

We compared the effects of DA modulation in our model to previously published reports. Hernández-López et al. (1997) reported that holding the cell at −82 mV (resting membrane potential) and activating D1 receptors (0.3-nA current injection, 300-ms duration) decreases spiking 62.5%. In our model, holding the cell at −87 mV, injecting 0.3-nA current for 300 ms, and simulating D1 modulation decreases spiking 20%. These authors also showed that holding the cell at −57 mV and activating D1 receptors increases spiking 34%, whereas in our model, holding the cell at −57 mV and simulating D1 modulation increase spiking 33%. Importantly, increasing the NaF modulation to a 17% reduction in conductance can match the 60% reduction in spiking reported by Hernández-López et al. (1997). Akaike et al. (1987) reported excitation after DA application that is sensitive to D2 receptor blockade. With a 0.3-nA current injection, they found that spiking is increased from 0 spikes per 300 ms to 5 spikes per 300 ms. In our model, D2 modulation increases spiking from 0 to 2 spikes (0.2375-nA injection). Accordingly, D1 excitation is the same in our model as in these experiments, whereas D1 inhibition and D2 excitation are somewhat more mild.

To explore the effects of D1R- and D2R-mediated modulation on the MSN response to synaptic input, we calculated the model spiking frequency versus synaptic input frequency (Fig. 3*B*; also see Supplementary Fig. 1 for examples of model response). We found that the model spikes in response to synaptic input frequencies in the range of 850–1,400 Hz, which corresponds very well with other reports of frequency values for "up-state generation" (806 ± 188 Hz: Blackwell et al. 2003; ≥600 Hz: Wilson 1992). As seen in the current injection experiments, the D1 Intrinsic condition induced a change in gain of the spiking response (Fig. 3*B*, solid red line) compared with the unmodulated response (Fig. 3*B*, black line) to synaptic input. At low synaptic input frequencies (<1,200

Hz), D1 Intrinsic modulation was inhibitory, whereas at frequencies >1,200 Hz D1 Intrinsic modulation became slightly excitatory. The D1 All condition significantly increased the spike frequency at all synaptic input frequencies (Fig. 3*B*, dashed red line) and slightly increased the change in gain beyond that in the D1 Intrinsic condition. Analogous to the current injection experiments, the D2 Intrinsic condition increased excitability of the cell in response to synaptic input (Fig. 3*B*, solid green line). The D2 All condition reduced the excitability of the model in response to synaptic input (Fig. 3*B*, dashed green line). Thus our results indicate that the net effect of D1R modulation is to excite MSN cells, whereas the net effect of D2R activation is to inhibit MSN cells in response to synaptic input.

Effects of dopamine MSN filtering of synaptic inputs

It has been suggested that DA might change the way that MSNs filter synaptic inputs, enhancing large synaptic inputs while filtering out smaller synaptic inputs (Bamford et al. 2004; Nicola et al. 2004). To investigate this possibility, we stimulated a tertiary dendrite with different-sized glutamatergic inputs while the cell was receiving synaptic input (1,050 Hz). We stimulated at a position located halfway out along the dendrite (Fig. 4*A*, *inset*). Evoked synaptic potential input sizes were expressed relative to a baseline conductance level from previous reports (Dalby and Mody 2003; Myme et al. 2003). Varying input size from 0.2- to 2.2-fold baseline revealed an approximately linear relationship between the size of the input and the measured somatic depolarization (Fig. 4*A*, black line). Neither D1 Intrinsic (Fig. 4*A*, solid red line) nor D2 Intrinsic (Fig. 4*A*, solid green line) modulation changed the linearity of this relationship significantly. Both conditions increased the magnitude of the depolarization measured at the soma, with larger inputs more enhanced relative to smaller inputs. Including synaptic effects diminished, but did not reverse, these relationships (D1 All, dashed red line; D2 All, dashed green line). The boost of inputs by D2 modulation was the result of an increase in sodium current; the boost by D1 modulation was mostly the result of decreased SK current (not shown).

We also examined the change in depolarization at the soma as a synaptic input was moved to progressively more distal locations on a tertiary dendrite (Fig. 4*B*, *inset*). D2 Intrinsic modulation again increased the magnitude of the depolarization measured at the soma for all distances (Fig. 4*B*, solid green curve) compared with the unmodulated condition (Fig. 4*B*, black curve), whereas D1 Intrinsic modulation appeared to have no effect (Fig. 4*B*, solid red curve). Including synaptic effects diminished this increase in magnitude for D2 modulation (D2 All, Fig. 4*B*, dashed green curve), but had no effect on D1 modulation (D1 All, Fig. 4*B*, dashed red curve). Based on these results, we conclude that DA modulation can preferentially enhance large inputs.

Dopamine and temporal integration properties of the MSN

Previous studies have shown that MSN somatic voltage appears to closely reflect integrated synaptic input over an approximately 50-ms timescale (Wolf et al. 2005b). We therefore investigated the possibility that DA modulation might change the integration time window of the MSN. We simulated a prolonged, nonspiking up-state and compared the resulting MSN somatic voltage (Fig. 5*A*, *top*, black trace) to the synaptic input frequency calculated using a sliding window of various widths (Fig. 5*A*, *top*, red trace). On calculating the covariance of the two (see METHODS), we found that the unmodulated MSN correlates best with input frequency binned over 50 ms (Fig. 5*B*, black trace). D1 Intrinsic modulation (Fig. 5*A*, *middle*) decreased the bin size with maximum correlation to 40 ms (Fig. 5*B*, solid red trace), whereas D2 Intrinsic modulation (Fig. 5*A*, *bottom*) increased the bin size with maximum correlation to 60 ms (Fig. 5*B*, solid green trace). Combining synaptic modulations with intrinsic modulations, as in the D1 and D2 All conditions, reversed this trend. D1 All modulation (Fig. 5*B*, dashed red trace) increased the bin size with maximum correlation to 60 ms, whereas D2 All modulation (Fig. 5*B*, dashed green trace) returned the bin size with maximum correlation to 50 ms.

We also investigated whether DA modulation affected the response of the model cell to inputs of different intensities and different degrees of coherence. First, we stimulated different numbers of glutamatergic synapses, randomly distributed throughout the cell, every 200 ms (Fig. 5*C*, *inset*), and calculated the probability of the stimulation eliciting a spike (see METHODS). Our results indicate that for the same stimulation (i.e., same set of synapses), D1 Intrinsic modulation (Fig. 5*C*, solid red trace) decreases the probability of the model spiking and D2 Intrinsic modulation (Fig. 5*C*, solid green trace) increases the probability of the model spiking in response to the stimulation, relative to the unmodulated condition (Fig. 5*C*, black trace). Combining synaptic modulations with intrinsic modulations reverses this trend. D1 All modulation (Fig. 5*C*, dashed red trace) increases the probability of the model spiking and D2 All modulation (Fig. 5*C*, dashed green trace) decreases the probability of the model spiking in response to the stimulation. Next, we examined how coherent these inputs needed to be to elicit a spike by varying the duration of the time window in which a given number of synapses was activated (Fig. 5*D*). As expected, increasing the duration of the time window generally decreased the probability of the model spiking in response to the stimulation. However, in general, D2 Intrinsic modulation increased the ability of the model to spike in response to wider stimulation windows (Fig. 5*D*, solid green line), whereas D1 Intrinsic modulation decreased this ability (Fig. 5*D*, solid red line), relative to the unmodulated condition (Fig. 5*D*, black line). Including synaptic modulations reversed this trend, with D1 All (Fig. 5*D*, dashed red line) modulation generally improving the ability of the cell to integrate temporally dispersed input and D2 All (Fig. 5*D*, dashed green line) modulation impairing this ability. These experiments suggest that DA modulation can alter the temporal integration properties of the MSN.

DISCUSSION

Dopaminergic modulation conditions

Historically, studies of the *net* effects of dopamine on MSN function have yielded a variety of results that are either conflicting or difficult to combine into a unifying hypothesis for dopaminergic modulation (Nicola et al. 2000), even though studies on individual channel modulations are mostly consis-

tent (Table 2). We used three approaches with our model in an attempt to integrate previous experimental results on the net effects of DA modulation. First, we used parameters derived from maximal physiological levels of dopaminergic modulation (Table 3) based strictly on previously published results (Table 2). Second, to be as objective as possible, we used modulation conditions that included all reported channel modulations for D1 or D2 receptors, rather than subjectively selecting certain channel modulations for inclusion in each subtype. Third, we applied modulation conditions to both a low-calcium (Wolf et al. 2005b) and a high-calcium tuned version of the MSN model. These tunings represent significantly different cells, yet both give the same results, suggesting that our findings may be generally true for MSN cells. Still, it will be necessary for future studies to thoroughly and systematically examine the full range of potential modulation conditions, applied to a number of distinctly tuned MSN cells, to ensure that this is the case.

We examined DA modulation of MSNs by breaking DA action down into either D1- or D2-receptor–mediated effects. Some MSNs may coexpress D1 and D2 receptors (Aizman et al. 2000; Surmeier et al. 1992, 1996). However, because D1 and D2 receptors mediate opposite effects on nearly every MSN channel (Table 3), we studied D1R- and D2R-mediated effects in isolation to most clearly illustrate their actions. It is possible that we were not able to capture the full effects of DA on the MSN by looking at solely D1R- or D2R-mediated effects—at least one study in ventral striatum has shown that D1 and D2 receptors on MSNs must be coactivated to modulate KAs (Hopf et al. 2003). However, the relative paucity of information on coactivation-dependent modulations prevents us from further addressing this possibility.

To examine the potential effects of various modulations, we created conditions incorporating results from studies in both dorsal and ventral striatum and applied these modulations to a model of the ventral striatal medium spiny neuron. Some reports have suggested that DA modulates ventral and dorsal cells differently (Nicola et al. 2000). However, a review of the literature on dopaminergic modulation of MSNs revealed that almost all studies in both dorsal and ventral striatum find consistent direction and magnitude of modulation for *individual* channels (see APPENDIX and Table 2 for more detail). Accordingly, we suggest that the data presented here are true for MSN cells from both dorsal and ventral striatum. Further study will be necessary to determine whether *net* DA modulation of MSNs is significantly different in the core, shell, and dorsal striatum.

DA has been shown to modulate GABAergic receptors in the striatum (Centonze et al. 2002; Flores-Hernández et al. 2000, 2002; Guzman et al. 2003; Hernández-Echeagaray et al. 2006; Hjelmstad 2004; Pennartz et al. 1992; Taverna et al. 2005). We do not include GABAergic modulation in this study for two reasons. First, as we reported previously (Wolf et al. 2005b), changes in the GABA conductance do not have an appreciable effect on the function of our model because of the way in which we have simulated GABAergic input as a desynchronized signal. Potentially, GABA inputs need to be synchronized to have a strong effect on MSN activity (Tepper et al. 2004). Second, DA appears to affect interneuron inputs and MSN collaterals differently; we do not distinguish between these two GABA sources in the present model. However, future studies will explore the effects of DA modulation of GABA on striatal network function.

Effects of D1R-mediated modulation on MSN nonlinearity and bistability

Bistability is the ability of a cell to remain in either of two membrane potentials indefinitely in the absence of external input. Because these states act as attractors, a bistable cell will exhibit a strongly nonlinear steady-state membrane potential profile in response to linear increases in synaptic input frequency (Fig. 2, *A* and *B*) because it will reside almost solely in these two states and switch abruptly between them. A bistable cell will also exhibit pronounced hysteresis, which is the characteristic of a cell to follow different voltage paths between two states depending on the direction of state transition (Fig. 2*D*)—this is caused by the tendency of the cell to maintain its current state as long as possible (Booth et al. 1997). In contrast, bimodality refers to a cell exhibiting two ranges (or modes) of membrane potentials (Fig. 2*C*), regardless of the mechanism (intrinsic properties or synaptic input). A bimodal cell may or may not also exhibit nonlinearity and hysteresis. The concept that MSNs might be bistable has been highly influential on functional theories of the basal ganglia. Several models of striatal/basal ganglia function have been built on the idea that striatal MSNs are inherently bistable, or become bistable after D1 modulation. Two of these models posit the basal ganglia as an action-selection mechanism, in which striatal MSN bistability enables the cortico-basal ganglionic loop to function as a pattern detector (Beiser and Houk 1998) or enhances the duration and intensity of striatal activity (Gruber et al. 2003). Another important model suggests that the ventral striatum gates cortical output based on limbic input, with MSNs transmitting information in the up-state but not in the down-state (Grace 2000; O'Donnell and Grace 1995). The concept that MSNs are intrinsically bistable arose from intracellular recordings performed in vivo in anesthetized animals, in which MSNs oscillate between spiking up-states and quiescent down-states with sharp transitions (Goto and O'Donnell 2001; Stern et al. 1997; Tseng et al. 2001; Wickens and Wilson 1998; Wilson and Kawaguchi 1996).

We did not observe bistability in our model, under any modulation condition (Fig. 2). The only condition in which we observed nonlinearity or bimodality was with a very high level of NMDA conductance [fivefold the baseline NMDA conductance, or an NMDA:AMPA (N:A) ratio of 2.5:1]. This observation agrees with a recent study in a two-compartment, MSN-like model that observes bimodality with a 4:1 N:A ratio (Kepecs and Raghavachari 2007). The exact N:A ratio in corticostriatal synapses can vary, but appear to remain below 1:1 in normal animals (Beurrier and Malenka 2002; Li et al. 2004; Popescu et al. 2007; Thomas et al. 2001), increasing to as high as 1.5:1 in cocaine-treated animals (Thomas et al. 2001). Studies of synapses onto cortical pyramidal neurons have found N:A ratios ranging from 0.2:1 to as high as 7.7:1 (Myme et al. 2003). However, the authors of this review note that studies of the N:A ratio using extracellularly evoked synaptic potentials/currents reliably report higher N:A ratios (probably because of suboptimal space clamping), as do studies using younger animals (p1–p15). Upon excluding these studies, the N:A ratios range from 0.2:1 to 1.2:1 (Myme et al.

2003). Taken together, these reports suggest that N:A ratios $\gtrsim$1.5:1 (which was not enough to induce bimodal behavior in our model) may not naturally occur in MSNs. We therefore suggest that NMDA-induced bistability is not likely to occur in MSNs under normal conditions. Because our model and others have suggested that the N:A ratio is extremely important in defining the behavioral response of MSNs to synaptic input and, because changes in this ratio have been hypothesized to occur in various disease states, it is crucial to further examine these ratios in adult animals in various areas of the striatum.

Although MSNs demonstrate bimodal membrane potentials under certain conditions, it is possible that this ability may not be functionally significant for striatal processing in the awake state. Recent in vivo intracellular recordings of MSNs found that although MSNs exhibited bimodal behavior during slow-wave sleep and anesthesia, the membrane potential distribution in the awake rat was clearly unimodal and centered at −61 mV (Mahon et al. 2006). In vivo studies in our lab have also indicated that in the awake state, hippocampal and cortical inputs to the accumbens sum sublinearly (Wolf et al. 2005a), not supralinearly, as would be expected if the bimodal membrane potential was responsible for a gating effect in the awake animal.

Effects of dopamine modulation on MSN excitability, filtering, and temporal integration

One influential hypothesis of basal ganglia function proposes that D1R activation excites MSN cells in the D1R-expressing, movement-facilitating, direct pathway, whereas D2R activation inhibits MSN cells in the D2R-expressing, movement-suppressing, indirect pathway (Albin et al. 1989; Delong 1990). We found that D1 modulation of intrinsic properties changed the slope of the frequency–current relationship, so that D1 intrinsic modulation could be inhibitory or excitatory, depending on the current injection amplitude (Fig. 3); simultaneous D1 modulation of both intrinsic and synaptic modulations was solely excitatory. Conversely, we found that D2 modulation of intrinsic properties was excitatory, although this was dependent on the direction and magnitude of sodium modulation, which is not precisely known; including synaptic modulations caused D2 modulation to be inhibitory. Accordingly, our results demonstrate that D1R-mediated modulation increases the activity of MSNs, whereas D2R-mediated modulation decreases the activity of MSNs (primarily as the result of synaptic modulations). This agrees with the classical model of the basal ganglia and supports the suggestion that loss of DA input to the striatum, as in Parkinson's disease, could alter the activity levels of D1- and D2-expressing MSNs and their downstream projections.

It has been suggested that dopamine acting at D1 receptors may differentially affect MSNs based on the current membrane potential, with hyperpolarized MSNs being inhibited and depolarized neurons being excited by D1R activation (Hernández-López et al. 1997; Nicola et al. 2000; Pacheco-Cano et al. 1996). We found that D1R activation changed the gain of the response of the MSN to current injection, so that at smaller current injections the MSN could be inhibited relative to the unmodulated state, whereas at larger current injections the cell could be excited (Fig. 3*A*). This gain change also occurred in response to synaptic input (Fig. 3*B*) and for both tunings of the cell (Supplementary Fig. 3). Accordingly, our findings support the possibility that D1R modulation of intrinsic properties might differentially affect the excitability of MSNs, exciting some while inhibiting others, based on the level of input to each MSN. It is important to note that simultaneous D1R modulation of both intrinsic and synaptic properties would be expected to solely cause MSN excitation, in agreement with the classical model of the basal ganglia.

It was previously proposed that dopamine may filter inputs to the MSN by enhancing the contrast between large and small synaptic inputs (Nicola et al. 2004). We found that DA modulation of intrinsic MSN properties enhanced the propagation of synaptic inputs to the soma, with larger synaptic inputs enhanced more than smaller ones (Fig. 4). However, including synaptic modulations diminished this effect. Still, the D2R-mediated up-regulation of sodium in the dendrites during D2 Intrinsic modulation should also increase backpropagation of action potentials into the dendrites, which would presumably affect the induction of synaptic plasticity in MSNs. However, these effects appear to be less significant than the effect of DA on MSN excitability.

We hypothesized that DA might affect the temporal integration properties of MSNs. Our results indicate that D1 modulation of intrinsic properties decreases the integration time window of the MSN, whereas D2 modulation of intrinsic properties increases this window. However, including synaptic effects again reverses this relationship, with the D1 All condition increasing the integration window and the D2 All condition returning the integration window to the unmodulated value. Regardless, the MSN appears to integrate synaptic inputs over a time window of 40 to 60 ms, suggesting that it functions more as an input integrator than as a classical coincidence detector. Given not only the very large number of glutamatergic inputs (5,000–15,000) each MSN receives, but also the ability of each MSN to respond to a minimum of 100 distinct cellular ensembles (Wolf et al. 2005b), this suggests that the MSN might function as a pattern detector, integrating and classifying patterns of cortical/subcortical inputs as part of the corticostriatal action selection mechanism. In this sense, dopaminergic modulation of the temporal integration window of MSNs might subtly regulate striatal integration of input from cortical ensembles.

Lack of synergy between intrinsic and synaptic effects

In all of the preceding cases, the synaptic effects of DA modulation counteracted the effects of DA modulation of intrinsic properties. Whether intrinsic and synaptic modulations always occur simultaneously is not known. However, it seems highly likely that both would occur at the same time because dopamine is a highly divergent signal, with one DA neuron targeting approximately 400 MSNs, 30% of DA neurons responding similarly to any given novel or salient event, and with the apparent ability of DA to diffuse out of the synaptic cleft (Arbuthnott and Wickens 2006; Hyland et al. 2002; Schultz 1998). One possibility is that the intrinsic and synaptic modulations counteract each other to maintain precisely balanced regulatory control over the MSN's integrative properties.

Another possibility is that both tonic and phasic dopamine release differentially affect intrinsic and synaptic properties

of the MSN. Dopamine neurons exhibit two basic activity modes—regular spiking and phasic bursting, which might initiate different downstream signaling mechanisms (Grace 1991). In this light, tonic spiking by DA neurons has been shown to maintain extrasynaptic DA levels at nanomolar concentrations, whereas bursting by DA neurons can boost DA concentration to micromolar levels, but possibly only within the synaptic cleft (Arbuthnott and Wickens 2006; Floresco et al. 2003; Phillips and Wightman 2004). Tonic, low-concentration DA levels might primarily influence intrinsic modulations at extrasynaptic sites, whereas phasic, high-concentration DA levels might control synaptic modulations. In this sense, the intrinsic effects of DA modulation could dominate during regular spiking, whereas the synaptic effects might override the intrinsic effects after short-term bursts by DA cells. Nonetheless, the intrinsic effects of DA modulation appear to be much less significant than the synaptic effects of DA modulation because the synaptic effects tended to dominate the net effect of DA modulation when the two were combined.

Possible D1-mediated regulation of calcium in dendritic spines

With the exception of its regulation of excitability, DA's effects on the integrative properties of the MSN appear to be surprisingly weak. Specifically, although we report that dopaminergic modulation can lead to changes in input filtering and temporal integration properties of the MSN, these effects do not appear to be very significant, at least at the single-cell level. Further, given that distinct MSN cells will inevitably express different levels and combinations of intrinsic and synaptic channels, it is even possible that dopamine may affect filtering and integration in opposite ways in different cells, even with the same modulation levels. Although we thoroughly examined multiple tunings of the model in an attempt to address this possibility, we did not systematically and rigorously examine the very large number of possible tunings for the model because this was outside the scope of this report. It is also important to note that despite our best efforts, the model is a simplified representation of a real cell and, as such, our findings will need to be confirmed and further explored in real cells. However, we suggest that in general, with the possible exception of DA's effects on MSN excitability by synaptic effects, dopamine may play only a minor role in MSN dendritic signal integration.

Rather than regulating the integrative properties of the medium spiny neuron at the whole cell or dendritic level we propose that DA modulation may function principally at spines, particularly during phasic DA release. The primary mechanism of action of this modulation may occur by D1 modulation regulating calcium influx into MSN dendritic spines. In Fig. 6, we outline a conceptual model in which the modulatory effects of D1R activation would interact to boost calcium influx through NMDA and L-type calcium channels. AMPA, NMDA, and L-type calcium channels are known to be located in the postsynaptic density (Olson et al. 2005). SK calcium-dependent channels are located in spine heads, where they have been shown to limit evoked synaptic potentials (Faber et al. 2005; Ngo-Anh et al. 2005). CaN and CaP/Q calcium channels regulate the SK current in MSNs, whereas L-type calcium channels do not (Vilchis et al. 2000). Sodium

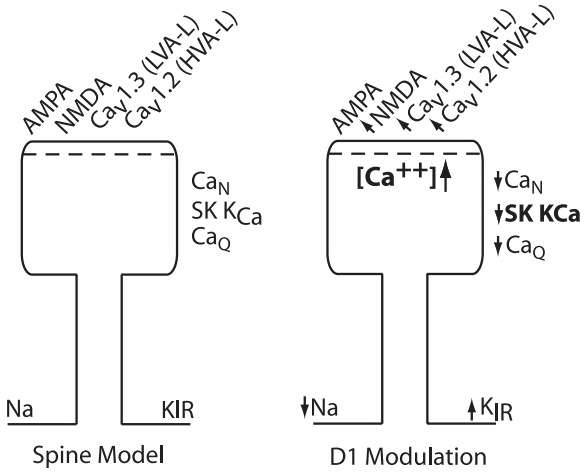

FIG. 6. Conceptual model of a dendritic spine in which D1 modulations of MSN intrinsic and synaptic channels interact cooperatively to boost calcium influx through NMDA and L-type calcium channels after synaptic activation. D1R-mediated up-regulation of NMDA and L-type channels in the postsynaptic density would directly boost calcium influx through these channels. D1R-mediated down-regulation of CaN and CaP/Q channels would indirectly boost calcium through NMDA and L-type calcium channels as well, by reducing SK calcium-dependent potassium activation—permitting greater depolarization of the spine head and therefore greater activation of NMDA and L-type channels. Because calcium through NMDA and L-type calcium channels is known to be important for the induction of synaptic plasticity, this could have major implications for regulation of long-term potentiation and long-term depression in the striatum. In this light, D1 modulations of KIR and sodium could represent a mechanism to maintain MSN excitability despite ongoing changes in synaptic strengths.

and KIR channels are most likely expressed in the dendrites of MSNs (Kerr and Plenz 2002; Pruss et al. 2003; Wilson 1992). Within this framework, D1R-mediated up-regulation of NMDA and L-type calcium channels would directly increase the amount of calcium entering the spine after synaptic activation. D1R-mediated down-regulation of CaN and CaP/Q channels would indirectly increase calcium influx through NMDA and L-type calcium channels still further because the associated reduction in SK activation would permit greater depolarization (and thus larger currents) after synaptic stimulation. Calcium currents through NMDA and L-type calcium channels have been shown to contribute to the induction of synaptic plasticity (Calabresi et al. 1994; Kapur et al. 1998; Olson et al. 2005; Yasuda et al. 2003); if this is the case, KIR and NaF modulation could regulate dendritic excitability in an activity-dependent manner, analogous to the I_h current in rat hippocampal neurons (Fan et al. 2005).

If true, dopaminergic regulation of spine-level calcium by modulation of MSN channels would provide a link between the extensive documentation of dopamine's modulatory effects at D1 receptors and its known role in controlling synaptic plasticity and guiding reinforcement learning. Should dopamine regulate synaptic plasticity in this manner, it is important to note that it could still regulate the integrative properties of the MSN as well. This control of integrative properties could entail any of the hypotheses we addressed herein. Our results suggest that dopamine most significantly affects MSN integration through its impact on excitability in the form of synaptic facilitation and inhibition.

We envision that dopamine acting at D1 receptors directly modulates NMDA channels to control synaptic facilitation

and inhibition. This represents a short-term regulatory mechanism that can significantly affect MSN excitability in response to synaptic input. Dopamine acting at D1 receptors also modulates several intrinsic MSN channels, which we suggest act cooperatively to regulate calcium influx to dendritic spines of the MSN. The resultant calcium influx might then determine the strength and direction of long-term synaptic potentiation and depression. In this manner, dopamine could significantly regulate striatal function at multiple timescales.

In conclusion, we investigated the effects of dopaminergic modulation on a model of the ventral striatal medium spiny neuron. By modeling the combined effects of DA on MSN intrinsic and synaptic channels, we were able to test three previously proposed hypotheses of DA function: *1*) that D1R activation enhances nonlinearity in the MSN; *2*) that DA acting on MSN D1Rs is excitatory, whereas DA acting on MSN D2Rs is inhibitory; and *3*) that DA preferably enhances the propagation of large synaptic inputs to the MSN soma. We also tested a fourth hypothesis, that DA changes the temporal integration properties of the MSN. We found that D1R-mediated modulation had no effect on nonlinearity in the MSN, nor was it able to induce bistability. Both D1 and D2 modulation affected excitability, input filtering, and the integration time window of the MSN model. However, in these cases, the effects of synaptic modulations counteracted the effects of intrinsic modulations and, in general, dominated the net effect of DA on MSN behavior. The observed lack of synergy between the intrinsic and synaptic effects led us to propose a mechanism in which all D1 modulations of MSN channels interact cooperatively to boost calcium influx through NMDA and L-type calcium channels at the spine level.

APPENDIX

As a rule, we used the maximum reported modulation level for each channel to maximize the likelihood of observing an effect on cell behavior. In some cases, however, the maximum modulation level led to unrealistic behavior (i.e., extreme changes in excitability, very wide action potentials, doublet spiking, etc.), and in these cases we used the largest modulations possible without incurring these behaviors.

D1R modulation of intrinsic channels

Although D1R activation has not been shown to directly modulate the KIR current in MSNs, D1R activation has been shown to decrease the resting input resistance 4–12% in dorsal and ventral striatum as well as to hyperpolarize the cell (Pacheco-Cano et al. 1996; Uchimura and North 1990; Uchimura et al. 1986). This is attributable to up-regulation of the inward-rectifying potassium current that is a hallmark of MSN cells (Nicola et al. 2000). Using the model, we determined that a 25% increase in the KIR current matched the reported changes in input resistance and hyperpolarization.

D1R activation was thought to modulate the KAs current (Surmeier and Kitai 1993). A later study suggested that this conductance change was the result of direct blockade of the KAs channel by SKF38393, the D1R agonist used (Nisenbaum et al. 1998). Additionally, another study found no D1R-mediated modulation of KAs (except when D2Rs were coactivated) (Hopf et al. 2003). Accordingly, we do not include D1 modulation of KAs in our study.

D1R agonists decrease ω-agatoxin (CaP/Q)– and ω-conotoxin GVIA (CaN)–sensitive currents in both dorsal and ventral striatal MSN cells (Salgado et al. 2005; Surmeier et al. 1995; Zhang et al. 2002). We calculated the approximate amount of reduction for the CaN and CaP/Q currents by assuming complete blockade of CaN channels by ω-conotoxin GVIA (CgTx) and of CaP/Q channels by ω-agatoxin (AgTx). In one study (Surmeier et al. 1995), AgTx and CgTx blocked 80% of the 70 pA (=56 pA) D1R-modulated current. CgTx alone blocked a mean of 40% of the D1R-modulated current, so the CgTx- and D1R-sensitive current is $0.4 \times 70 = 28$ pA. This suggests that the AgTx- and D1R-sensitive current is $56 - 28 = 28$ pA. The total AgTx- and CgTx-sensitive current is reported as 90 pA; previous studies have shown that the approximate ratio of CgTx:AgTx-sensitive currents is 5:3 (Churchill and Macvicar 1998). Applying this ratio gives whole cell values of 56.3 pA for CgTx-sensitive and 33.8 pA for AgTx-sensitive currents. This gives a percentage blockade by D1R activation of 28 pA/56.3 pA = 50% for CgTx-sensitive (CaN) and 28 pA/33.8 pA = 83% for AgTx-sensitive (CaP/Q) currents. In the same manner, we calculated broadly similar values in other studies (Salgado et al. 2005; Zhang et al. 2002). We use a modulated conductance level of 20% of the unmodulated conductance for the CaP/Q and 50% for the CaN (Table 3). At least one study has shown that DA decreased the interspike interval of cells during trains of action potentials (Rutherford et al. 1988). We suggest that this reflects decreased SK current as a result of DA modulation of CaN and CaP/Q channels.

D1R agonist application has been reported to reduce the conductance of the fast sodium current by 22–37.8% (Table 2) (Calabresi et al. 1987; Schiffmann et al. 1995, 1998; Surmeier et al. 1992; Zhang et al. 1998). The NaF inactivation curve may also be shifted up to −5.6 mV (Surmeier et al. 1992). We model D1R-mediated modulation of sodium current as a 5% reduction of the total conductance, without a shift in the inactivation curve. Decreasing the conductance any further, or shifting the inactivation curve with the 5% reduction, seriously reduces spiking in response to current injection. This seems inappropriate given that D1R activation does not completely shut down cell spiking. Dopamine has also been reported to regulate persistent sodium current, although it is not known whether this is a D1R- or D2R-mediated modulation (Cepeda et al. 1995). For this reason, we do not include this modulation in our studies. Still, we did investigate the potential effects that NaP regulation would have on both D1 and D2 conditions and found that even a complete blockade of the NaP current had no effect on any of the studies described herein.

D1R agonists are known to up-regulate L-type calcium channels (Nicola et al. 2000; Song and Surmeier 1996; Surmeier et al. 1995), but the exact modulations have not been published. D1R stimulation may either increase the maximum conductance of the Cav1.3 (up to twofold) or it may shift the activation of the Cav1.3 between −5 and −15 mV (Surmeier et al. 1995). To explore these conditions, we compared a doubling of the Cav1.3 current and a −10-mV shift of the activation curve for the Cav1.3 to the unmodulated cell in response to a 0.271-nA current injection (data not shown). Doubling the whole cell Cav1.3 current has

little effect on MSN spike frequency, whereas shifting the Cav1.3 activation by −10 mV increases spike frequency. This is because in the shifted condition, the Cav1.3 is able to contribute much more significantly to the subthreshold behavior of the cell. Increasing the Cav1.3 current more than twofold resulted in aberrant spiking—spike doublets and delayed spike repolarization—as did shifting the Cav1.3 more than −15 mV. Accordingly, we model D1 modulation of the Cav1.3 channel as a −10-mV shift in the activation kinetics of the channel. D1 appears to either shift Cav1.2 channels −10 to −15 mV or increase the conductance by ≤100%. Shifting the Cav1.2 is equivalent to increasing the Cav1.3 conductance; therefore we increased the conductance of the Cav1.2 instead.

D1R modulation of synaptic channels

In the following discussion, we do not differentiate between pre- and postsynaptic effects of dopamine. Presumably, because the studies that we cite are recording synaptically evoked potentials in the MSN and stimulating presynaptically, the effects reported should include both pre- and postsynaptic contributions. Five of seven studies (one in ventral striatum) found that D1 modulation enhanced NMDA current 3–41% (Cepeda et al. 1998; Flores-Hernández et al. 2002; Hallett et al. 2006; Harvey and Lacey 1997; Levine et al. 1996). Two studies found decreased NMDA current with D1R stimulation. One of these was performed in fetal cells (Castro et al. 1999), in which case the expression of NMDA may not reflect adult expression levels or type. The second was performed on acutely dissociated cells (Yasuda et al. 2003). Glutamatergic input to MSNs is almost wholly located on the dendrites (Wilson 1992), so this result may not reflect NMDA modulation in the intact animal. Given these findings, it appears safe to conclude that D1R-mediated modulation increases NMDA current and to model it with a 30% increase in conductance.

D1R activation increased AMPA current in two studies in dorsal striatum (Price et al. 1999; Umemiya and Raymond 1997), had no effect in another (Levine et al. 1996), and decreased AMPA in one study in ventral striatum (Harvey and Lacey 1996). Given these conflicting results, we assume that D1 does not significantly or consistently modulate AMPA in either direction.

D2R modulation of intrinsic channels

The results of D2R activation on sodium currents are mixed (Hu et al. 2005; Surmeier et al. 1992; White et al. 1997; Zhang et al. 1998). A study in dorsal striatum found that D2R agonists increased sodium conductance by 20% with a +5-mV shift in the inactivation curve in the whole cell recording mode (Surmeier et al. 1992). However, in the cell-attached recording mode D2R agonists did not change conductance levels but did shift the inactivation voltage −16.9 mV. The authors suggest that the cell-attached mode constitutes a membrane-delimited mechanism and represents D3R modulation, whereas the whole cell mode represents D2R modulation (because D2R-mediated modulation requires second messengers). To our knowledge, this has still not been further investigated. We found that the direction of shift of the sodium inactivation curve critically determines whether D2 modulation is excitatory or inhibitory. Several groups have reported that D2R-mediated modulation of intrinsic channels results in increased excitability of the cell in response to current injection (Akaike et al. 1987; Higashi et al. 1989; Yim and Mogenson 1988) and NaF conductance increased 25% in a ventral striatal study (Hu et al. 2005). Therefore we presume that D2R activation increases NaF conductance and model D2R modulation of sodium with a 10% increase in current and +5-mV shift in the inactivation curve. The exact modulation of NaF by D2R activation needs to be better explored, especially because this modulation dominates the effects of D2 modulation of intrinsic properties.

D2R modulation of synaptic channels

Four of four studies show no change in NMDA current after D2R stimulation (Cepeda et al. 1998; Flores-Hernández et al. 2002; Levine et al. 1996; Lin et al. 2003). Two studies found decreased AMPA current during D2 modulation (Hernández-Echeagaray et al. 2004; Levine et al. 1996) and at least five more studies found that D2 application decreased glutamatergic response (Bamford et al. 2004; Goto and Grace 2005a,b; Hsu et al. 1995; Yim and Mogenson 1988). Recent studies have indicated that D2 modulates glutamatergic response by a presynaptic mechanism (Bamford et al. 2004; Goto and Grace 2005b). Irrespective of whether the mechanism is presynaptic, it appears that D2 modulation reduces glutamatergic response and may be best modeled as a reduction in the AMPA component. This was implemented as a 20% reduction in the AMPA conductance with no change in NMDA.

Exploration of the modulation parameter space

We explored most of the modulation parameter space by hand and were unable to find modulation conditions for which the main results discussed herein changed. For example, for D1, we examined at least four different combinations of CaN and CaP/Q modulations, eight different combinations of NaF conductance and voltage shift modulations, several types of CaL modulation, at least six modulation levels with the KIR channel, at least five modulation levels with the NMDA channel, one or two modulation levels with the AMPA channel, and a few with the KAs channel. For D2, we examined the effects of NaF modulation using several combinations of conductance and voltage shift parameters, two to three modulation levels with the KAs channel, at least three or four levels with the KIR channel, and three to four levels with the AMPA channel. We also combined the modulations in several different ways to examine the effects of individual channels on the net effects of the modulation condition; for example, for D1, we tried just calcium modulations, just inhibitory modulations, just excitatory modulations, just NaF and KIR, just CaL and KIR, just intrinsic modulations, and just synaptic modulations. For D2, we examined just inhibitory modulations, just excitatory modulations, just NaF and KAs, just intrinsic modulations, and just synaptic modulations.

ACKNOWLEDGMENTS

We thank P. O'Donnell and M. Benoit-Marand for in vitro cell recordings and W. Hopf for helpful discussion of the manuscript.

GRANTS

This work was supported by National Institute of Mental Health Conte Center Grant MH-064045.

REFERENCES

Aizman O, Brismar H, Uhlen P, Zettergren E, Levey AI, Forssberg H, Greengard P, Aperia A. Anatomical and physiological evidence for D1 and D2 dopamine receptor colocalization in neostriatal neurons. *Nat Neurosci* 3: 226–230, 2000.

Akaike A, Ohno Y, Sasa M, Takaori S. Excitatory and inhibitory effects of dopamine on neuronal activity of the caudate nucleus neurons in vitro. *Brain Res* 418: 262–272, 1987.

Albin RL, Young AB, Penney JB. The functional anatomy of basal ganglia disorders. *Trends Neurosci* 12: 366–375, 1989.

Arbuthnott GW, Wickens J. Space, time and dopamine. *Trends Neurosci* 30: 62–69, 2006.

Bamford NS, Zhang H, Schmitz Y, Wu NP, Cepeda C, Levine MS, Schmauss C, Zakharenko SS, Zablow L, Sulzer D. Heterosynaptic dopamine neurotransmission selects sets of corticostriatal terminals. *Neuron* 42: 653–663, 2004.

Bargas J, Howe A, Eberwine J, Cao Y, Surmeier DJ. Cellular and molecular characterization of Ca^{2+} currents in acutely isolated, adult rat neostriatal neurons. *J Neurosci* 14: 6667–6686, 1994.

Beiser D, Houk J. Model of cortical-basal ganglionic processing: encoding the serial order of sensory events. *J Neurophysiol* 79: 3168–3188, 1998.

Beurrier C, Malenka RC. Enhanced inhibition of synaptic transmission by dopamine in the nucleus accumbens during behavioral sensitization to cocaine. *J Neurosci* 22: 5817–5822, 2002.

Blackwell KT, Czubayko U, Plenz D. Quantitative estimate of synaptic inputs to striatal neurons during up and down states in vitro. *J Neurosci* 23: 9123–9132, 2003.

Booth V, Rinzel J, Kiehn O. Compartmental model of vertebrate motoneurons for Ca^{2+}-dependent spiking and plateau potentials under pharmacological treatment. *J Neurophysiol* 78: 3371–3385, 1997.

Burnashev N, Zhou Z, Neher E, Sakmann B. Fractional calcium currents through recombinant GluR channels of the NMDA, AMPA and kainate receptor subtypes. *J Physiol* 485: 403–418, 1995.

Calabresi P, Mercuri N, Stanzione P, Stefani A, Bernardi G. Intracellular studies on the dopamine-induced firing inhibition of neostriatal neurons in vitro: evidence for D1 receptor involvement. *Neuroscience* 20: 757–771, 1987.

Calabresi P, Pisani A, Mercuri NB, Bernardi G. Post-receptor mechanisms underlying striatal long-term depression. *J Neurosci* 14: 4871–4881, 1994.

Carnevale NT, Hines ML. *The NEURON Book.* New York: Cambridge Univ. Press, 2005.

Carter AG, Sabatini BL. State-dependent calcium signaling in dendritic spines of striatal medium spiny neurons. *Neuron* 44: 483–493, 2004.

Castro NG, de Mello MC, de Mello FG, Aracava Y. Direct inhibition of the N-methyl-D-aspartate receptor channel by dopamine and (+)-SKF38393. *Br J Pharmacol* 126: 1847–1855, 1999.

Centonze D, Picconi B, Baunez C, Borrelli E, Pisani A, Bernardi G, Calabresi P. Cocaine and amphetamine depress striatal GABAergic synaptic transmission through D2 dopamine receptors. *Neuropsychopharmacology* 26: 164–175, 2002.

Cepeda C, Chandler SH, Shumate LW, Levine MS. Persistent Na^{+} conductance in medium-sized neostriatal neurons: characterization using infrared videomicroscopy and whole cell patch-clamp recordings. *J Neurophysiol* 74: 1343–1348, 1995.

Cepeda C, Colwell CS, Itri JN, Chandler SH, Levine MS. Dopaminergic modulation of NMDA-induced whole cell currents in neostriatal neurons in slices: contribution of calcium conductances. *J Neurophysiol* 79: 82–94, 1998.

Cepeda C, Levine MS. Dopamine and N-methyl-D-aspartate receptor interactions in the neostriatum. *Dev Neurosci* 20: 1–18, 1998.

Chapman DE, Keefe KA, Wilcox KS. Evidence for functionally distinct synaptic NMDA receptors in ventromedial versus dorsolateral striatum. *J Neurophysiol* 89: 69–80, 2003.

Churchill D, Macvicar BA. Biophysical and pharmacological characterization of voltage-dependent Ca^{2+} channels in neurons isolated from rat nucleus accumbens. *J Neurophysiol* 79: 635–647, 1998.

Coetzee WA, Amarillo Y, Chiu J, Chow A, Lau D, McCormack T, Moreno H, Nadal MS, Ozaita A, Pountney D, Saganich M, Vega-Saenz de Miera E, Rudy B. Molecular diversity of K^{+} channels. *Ann NY Acad Sci* 868: 233–285, 1999.

Dalby NO, Mody I. Activation of NMDA receptors in rat dentate gyrus granule cells by spontaneous and evoked transmitter release. *J Neurophysiol* 90: 786–797, 2003.

Day M, Wang Z, Ding J, An X, Ingham CA, Shering AF, Wokosin D, Ilijic E, Sun Z, Sampson AR, Mugnaini E, Deutch AY, Sesack SR, Arbuthnott GW, Surmeier DJ. Selective elimination of glutamatergic synapses on striatopallidal neurons in Parkinson disease models. *Nat Neurosci* 9: 251–259, 2006.

Delong M. Primate models of movement disorders of basal ganglia origin. *Trends Neurosci* 13: 281–285, 1990.

Erisir A, Lau D, Rudy B, Leonard CS. Function of specific K(+) channels in sustained high-frequency firing of fast-spiking neocortical interneurons. *J Neurophysiol* 82: 2476–2489, 1999.

Faber ES, Delaney AJ, Sah P. SK channels regulate excitatory synaptic transmission and plasticity in the lateral amygdala. *Nat Neurosci* 8: 635–641, 2005.

Fan Y, Fricker D, Brager DH, Chen X, Lu HC, Chitwood RA, Johnston D. Activity-dependent decrease of excitability in rat hippocampal neurons through increases in I(h). *Nat Neurosci* 8: 1542–1551, 2005.

Flores-Hernández J, Cepeda C, Hernández-Echeagaray E, Calvert CR, Jokel ES, Fienberg AA, Greengard P, Levine MS. Dopamine enhancement of NMDA currents in dissociated medium-sized striatal neurons: role of D1 receptors and DARPP-32. *J Neurophysiol* 88: 3010–3020, 2002.

Flores-Hernández J, Hernández S, Snyder GL, Yan Z, Fienberg AA, Moss SJ, Greengard P, Surmeier DJ. D(1) dopamine receptor activation reduces GABA(A) receptor currents in neostriatal neurons through a PKA/DARPP-32/PP1 signaling cascade. *J Neurophysiol* 83: 2996–3004, 2000.

Floresco SB, West AR, Ash B, Moore H, Grace AA. Afferent modulation of dopamine neuron firing differentially regulates tonic and phasic dopamine transmission. *Nat Neurosci* 6: 968–973, 2003.

Fujiyama F, Fritschy JM, Stephenson FA, Bolam JP. Synaptic localization of GABA(A) receptor subunits in the striatum of the rat. *J Comp Neurol* 416: 158–172, 2000.

Galarreta M, Hestrin S. Properties of GABAA receptors underlying inhibitory synaptic currents in neocortical pyramidal neurons. *J Neurosci* 17: 7220–7227, 1997.

Gerfen CR, Engber TM, Mahan LC, Susel Z, Chase TN, Monsma FJ Jr, Sibley DR. D1 and D2 dopamine receptor-regulated gene expression of striatonigral and striatopallidal neurons. *Science* 250: 1429–1432, 1990.

Gonon F. Prolonged and extrasynaptic excitatory action of dopamine mediated by D1 receptors in the rat striatum in vivo. *J Neurosci* 17: 5972–5978, 1997.

Goto Y, Grace AA. Dopamine-dependent interactions between limbic and prefrontal cortical plasticity in the nucleus accumbens: disruption by cocaine sensitization. *Neuron* 47: 255–266, 2005a.

Goto Y, Grace AA. Dopaminergic modulation of limbic and cortical drive of nucleus accumbens in goal-directed behavior. *Nat Neurosci* 8: 805–812, 2005b.

Goto Y, O'Donnell P. Network synchrony in the nucleus accumbens in vivo. *J Neurosci* 21: 4498–4504, 2001.

Gotz T, Kraushaar U, Geiger J, Lubke J, Berger T, Jonas P. Functional properties of AMPA and NMDA receptors expressed in identified types of basal ganglia neurons. *J Neurosci* 17: 204–215, 1997.

Grace AA. Phasic versus tonic dopamine release and the modulation of dopamine system responsivity: a hypothesis for the etiology of schizophrenia. *Neuroscience* 41: 1–24, 1991.

Grace AA. Gating of information flow within the limbic system and the pathophysiology of schizophrenia. *Brain Res Brain Res Rev* 31: 330–341, 2000.

Gracy KN, Clarke CL, Meyers MB, Pickel VM. N-Methyl-D-aspartate receptor 1 in the caudate-putamen nucleus: ultrastructural localization and co-expression with sorcin, a 22,000 mol. wt calcium binding protein. *Neuroscience* 90: 107–117, 1999.

Gruber AJ, Solla SA, Surmeier DJ, Houk JC. Modulation of striatal single units by expected reward: a spiny neuron model displaying dopamine-induced bistability. *J Neurophysiol* 90: 1095–1114, 2003.

Guzman JN, Hernández A, Galarraga E, Tapia D, Laville A, Vergara R, Aceves J, Bargas J. Dopaminergic modulation of axon collaterals interconnecting spiny neurons of the rat striatum. *J Neurosci* 23: 8931–8940, 2003.

Hallett PJ, Spoelgen R, Hyman BT, Standaert DG, Dunah AW. Dopamine D1 activation potentiates striatal NMDA receptors by tyrosine phosphorylation-dependent subunit trafficking. *J Neurosci* 26: 4690–4700, 2006.

Harvey J, Lacey MG. Endogenous and exogenous dopamine depress EPSCs in rat nucleus accumbens in vitro via D1 receptors activation. *J Physiol* 492: 143–154, 1996.

Harvey J, Lacey MG. A postsynaptic interaction between dopamine D1 and NMDA receptors promotes presynaptic inhibition in the rat nucleus accumbens via adenosine release. *J Neurosci* 17: 5271–5280, 1997.

Hernández-Echeagaray E, Cepeda C, Ariano MA, Lobo MK, Sibley DR, Levine MS. Dopamine reduction of GABA currents in striatal medium-sized spiny neurons is mediated principally by the D_1 receptor subtype. *Neurochem Res* 32: 229–240, 2006.

Hernández-Echeagaray E, Starling AJ, Cepeda C, Levine MS. Modulation of AMPA currents by D2 dopamine receptors in striatal medium-sized spiny neurons: are dendrites necessary? *Eur J Neurosci* 19: 2455–2463, 2004.

Hernández-López S, Bargas J, Surmeier DJ, Reyes A, Galarraga E. D1 receptor activation enhances evoked discharge in neostriatal medium spiny neurons by modulating an L-type Ca^{2+} conductance. *J Neurosci* 17: 3334–3342, 1997.

Higashi H, Inanaga K, Nishi S, Uchimura N. Enhancement of dopamine actions on rat nucleus accumbens neurones in vitro after methamphetamine pre-treatment. *J Physiol* 408: 587–603, 1989.

Hines ML, Carnevale NT. The NEURON simulation environment. *Neural Comput* 9: 1179–1209, 1997.

Hjelmstad GO. Dopamine excites nucleus accumbens neurons through the differential modulation of glutamate and GABA release. *J Neurosci* 24: 8621–8628, 2004.

Hoehn K, Watson TW, MacVicar BA. Multiple types of calcium channels in acutely isolated rat neostriatal neurons. *J Neurosci* 13: 1244–1257, 1993.

Hopf FW, Maria Grazia C, Adrienne SG, Ivan D, Antonello B. Cooperative activation of dopamine D1 and D2 receptors increases spike firing of nucleus accumbens neurons via G-protein betagamma subunits. *J Neurosci* 23: 5079–5087, 2003.

Houk JC. Information processing in modular circuits linking basal ganglia and cerebral cortex. In: *Models of Information Processing in the Basal Ganglia*, edited by Houk JC, Davis JL, Beiser DG. Cambridge, MA: The MIT Press, 1995, p. 3–9.

Hsu KS, Huang CC, Yang CH, Gean PW. Presynaptic D2 dopaminergic receptors mediate inhibition of excitatory synaptic transmission in rat neostriatum. *Brain Res* 690: 264–268, 1995.

Hu XT, Dong Y, Zhang XF, White FJ. Dopamine D2 receptor-activated Ca^{2+} signaling modulates voltage-sensitive sodium currents in rat nucleus accumbens neurons. *J Neurophysiol* 93: 1406–1417, 2005.

Hyland BI, Reynolds JN, Hay J, Perk CG, Miller R. Firing modes of midbrain dopamine cells in the freely moving rat. *Neuroscience* 114: 475–492, 2002.

Kapur A, Yeckel MF, Gray R, Johnston D. L-Type calcium channels are required for one form of hippocampal mossy fiber LTP. *J Neurophysiol* 79: 2181–2190, 1998.

Kepecs A, Raghavachari S. Gating information by two-state membrane potential fluctuations. *J Neurophysiol* 97: 3015–3023, 2007.

Kerr JN, Plenz D. Dendritic calcium encodes striatal neuron output during up-states. *J Neurosci* 22: 1499–1512, 2002.

Kerr JN, Plenz D. Action potential timing determines dendritic calcium during striatal up-states. *J Neurosci* 24: 877–885, 2004.

Le Moine C, Bloch B. Expression of the D3 dopamine receptor in peptidergic neurons of the nucleus accumbens: comparison with the D1 and D2 dopamine receptors. *Neuroscience* 73: 131–143, 1996.

Levine MS, Li Z, Cepeda C, Cromwell HC, Altemus KL. Neuromodulatory actions of dopamine on synaptically-evoked neostriatal responses in slices. *Synapse* 24: 65–78, 1996.

Li L, Murphy TH, Hayden MR, Raymond LA. Enhanced striatal NR2B-containing *N*-methyl-D-aspartate receptor-mediated synaptic currents in a mouse model of Huntington disease. *J Neurophysiol* 92: 2738–2746, 2004.

Lin JY, Dubey R, Funk GD, Lipski J. Receptor subtype-specific modulation by dopamine of glutamatergic responses in striatal medium spiny neurons. *Brain Res* 959: 251–262, 2003.

Mahon S, Vautrelle N, Pezard L, Slaght SJ, Deniau JM, Chouvet G, Charpier S. Distinct patterns of striatal medium spiny neuron activity during the natural sleep-wake cycle. *J Neurosci* 26: 12587–12595, 2006.

Maurice N, Deniau JM, Glowinski J, Thierry AM. Relationships between the prefrontal cortex and the basal ganglia in the rat: physiology of the cortico-nigral circuits. *J Neurosci* 19: 4674–4681, 1999.

Myme CI, Sugino K, Turrigiano GG, Nelson SB. The NMDA-to-AMPA ratio at synapses onto layer 2/3 pyramidal neurons is conserved across prefrontal and visual cortices. *J Neurophysiol* 90: 771–779, 2003.

Ngo-Anh TJ, Bloodgood BL, Lin M, Sabatini BL, Maylie J, Adelman JP. SK channels and NMDA receptors form a Ca^{2+}-mediated feedback loop in dendritic spines. *Nat Neurosci* 8: 642–649, 2005.

Nicola SM, Surmeier J, Malenka RC. Dopaminergic modulation of neuronal excitability in the striatum and nucleus accumbens. *Annu Rev Neurosci* 23: 185–215, 2000.

Nicola SM, Woodward Hopf F, Hjelmstad GO. Contrast enhancement: a physiological effect of striatal dopamine? *Cell Tissue Res* 318: 93–106, 2004.

Nisenbaum ES, Mermelstein PG, Wilson CJ, Surmeier DJ. Selective blockade of a slowly inactivating potassium current in striatal neurons by (±)-6-chloro-APB hydrobromide (SKF82958). *Synapse* 29: 213–224, 1998.

Nisenbaum ES, Wilson CJ, Foehring RC, Surmeier DJ. Isolation and characterization of a persistent potassium current in neostriatal neurons. *J Neurophysiol* 76: 1180–1194, 1996.

Nusser Z, Hajos N, Somogyi P, Mody I. Increased number of synaptic GABA(A) receptors underlies potentiation at hippocampal inhibitory synapses. *Nature* 395: 172–177, 1998.

Obermair GJ, Kaufmann WA, Knaus HG, Flucher BE. The small conductance Ca^{2+}-activated K^+ channel SK3 is localized in nerve terminals of excitatory synapses of cultured mouse hippocampal neurons. *Eur J Neurosci* 17: 721–731, 2003.

O'Donnell P, Grace AA. Physiological and morphological properties of accumbens core and shell neurons recorded in vitro. *Synapse* 13: 135–160, 1993.

O'Donnell P, Grace AA. Synaptic interactions among excitatory afferents to nucleus accumbens neurons: hippocampal gating of prefrontal cortical input. *J Neurosci* 15: 3622–3639, 1995.

Olson PA, Tkatch T, Hernández-López S, Ulrich S, Ilijic E, Mugnaini E, Zhang H, Bezprozvanny I, Surmeier DJ. G-protein-coupled receptor modulation of striatal CaV1.3 L-type Ca^{2+} channels is dependent on a Shank-binding domain. *J Neurosci* 25: 1050–1062, 2005.

Pacheco-Cano MT, Bargas J, Hernández-López S, Tapia D, Galarraga E. Inhibitory action of dopamine involves a subthreshold Cs(+)-sensitive conductance in neostriatal neurons. *Exp Brain Res* 110: 205–211, 1996.

Pennartz CM, Dolleman-van der Weel MJ, Kitai ST, Lopes da Silva FH. Presynaptic dopamine D1 receptors attenuate excitatory and inhibitory limbic inputs to the shell region of the rat nucleus accumbens studied in vitro. *J Neurophysiol* 67: 1325–1334, 1992.

Perez MF, White FJ, Hu XT. Dopamine D2 receptor modulation of K^+ channel activity regulates excitability of nucleus accumbens neurons at different membrane potentials. *J Neurophysiol* 96: 2217–2228, 2006.

Phillips PE, Wightman RM. Extrasynaptic dopamine and phasic neuronal activity (Letter). *Nat Neurosci* 7: 199; author reply 199, 2004.

Pickel VM, Heras A. Ultrastructural localization of calbindin-D28k and GABA in the matrix compartment of the rat caudate-putamen nuclei. *Neuroscience* 71: 167–178, 1996.

Popescu AT, Saghyan AA, Paré D. NMDA-dependent facilitation of corticostriatal plasticity by the amygdala. *Proc Natl Acad Sci USA* 104: 341–346, 2007.

Price CJ, Kim P, Raymond LA. D1 dopamine receptor-induced cyclic AMP-dependent protein kinase phosphorylation and potentiation of of striatal glutamate receptors. *J Neurochem* 73: 2441–2446, 1999.

Pruss H, Wenzel M, Eulitz D, Thomzig A, Karschin A, Veh RW. Kir2 potassium channels in rat striatum are strategically localized to control basal ganglia function. *Brain Res Mol Brain Res* 110: 203–219, 2003.

Russell SN, Publicover NG, Hart PJ, Carl A, Hume JR, Sanders KM, Horowitz B. Block by 4-aminopyridine of a Kv1.2 delayed rectifier K^+ current expressed in Xenopus oocytes. *J Physiol* 481: 571–584, 1994.

Rutherford A, Garcia-Munoz M, Arbuthnott GW. An afterhyperpolarization recorded in striatal cells "in vitro": effect of dopamine administration. *Exp Brain Res* 71: 399–405, 1988.

Salgado H, Tecuapetla F, Perez-Rosello T, Perez-Burgos A, Perez-Garci E, Galarraga E, Bargas J. A reconfiguration of CaV2 Ca^{2+} channel current and its dopaminergic D2 modulation in developing neostriatal neurons. *J Neurophysiol* 94: 3771–3787, 2005.

Schiffmann SN, Desdouits F, Menu R, Greengard P, Vincent JD, Vanderhaeghen JJ, Girault JA. Modulation of the voltage-gated sodium current in rat striatal neurons by DARPP-32, an inhibitor of protein phosphatase. *Eur J Neurosci* 10: 1312–1320, 1998.

Schiffmann SN, Lledo PM, Vincent JD. Dopamine D1 receptor modulates the voltage-gated sodium current in rat striatal neurones through a protein kinase A. *J Physiol* 483: 95–107, 1995.

Schiller J, Schiller Y. NMDA receptor-mediated dendritic spikes and coincident signal amplification. *Curr Opin Neurobiol* 11: 343–348, 2001.

Schultz W. Predictive reward signal of dopamine neurons. *J Neurophysiol* 80: 1–27, 1998.

Segev I, Burke RE. Compartmental models of complex neurons. In: *Methods in Neuronal Modeling: From Ions to Networks* (2nd ed.), edited by Koch C, Segev I. Cambridge, MA: MIT Press, 1998, p. 93–136.

Shen W, Hernández-López S, Tkatch T, Held JE, Surmeier DJ. Kv1.2-containing K^+ channels regulate subthreshold excitability of striatal medium spiny neurons. *J Neurophysiol* 91: 1337–1349, 2004.

Song WJ, Surmeier DJ. Voltage-dependent facilitation of calcium channels in rat neostriatal neurons. *J Neurophysiol* 76: 2290–2306, 1996.

Song WJ, Tkatch T, Baranauskas G, Ichinohe N, Kitai ST, Surmeier DJ. Somatodendritic depolarization-activated potassium currents in rat neostriatal cholinergic interneurons are predominantly of the A type and attributable to coexpression of Kv4.2 and Kv4.1 subunits. *J Neurosci* 18: 3124–3137, 1998.

Stern EA, Kincaid AE, Wilson CJ. Spontaneous subthreshold membrane potential fluctuations and action potential variability of rat corticostriatal and striatal neurons in vivo. *J Neurophysiol* 77: 1697–1715, 1997.

Surmeier DJ, Bargas J, Hemmings HC, Nairn AC, Greengard P. Modulation of calcium currents by a D1 dopaminergic protein kinase/phosphatase cascade in rat neostriatal neurons. *Neuron* 14: 385–397, 1995.

Surmeier DJ, Eberwine J, Wilson CJ, Cao Y, Stefani A, Kitai ST. Dopamine receptor subtypes colocalize in rat striatonigral neurons. *Proc Natl Acad Sci USA* 89: 10178–10182, 1992.

Surmeier DJ, Kitai ST. D1 and D2 dopamine receptor modulation of sodium and potassium currents in rat neostriatal neurons. *Prog Brain Res* 99: 309–324, 1993.

Surmeier DJ, Song WJ, Yan Z. Coordinated expression of dopamine receptors in neostriatal medium spiny neurons. *J Neurosci* 16: 6579–6591, 1996.

Taverna S, Canciani B, Pennartz CMA. Dopamine D1-receptors modulate lateral inhibition between principal cells of the nucleus accumbens. *J Neurophysiol* 93: 1816–1819, 2005.

Tepper JM, Koos T, Wilson CJ. GABAergic microcircuits in the neostriatum. *Trends Neurosci* 27: 662–669, 2004.

Thomas MJ, Beurrier C, Bonci A, Malenka RC. Long-term depression in the nucleus accumbens: a neural correlate of behavioral sensitization to cocaine. *Nat Neurosci* 4: 1217–1223, 2001.

Tseng KY, Kasanetz F, Kargieman L, Riquelme LA, Murer MG. Cortical slow oscillatory activity is reflected in the membrane potential and spike trains of striatal neurons in rats with chronic nigrostriatal lesions. *J Neurosci* 21: 6430–6439, 2001.

Uchimura N, Higashi H, Nishi S. Hyperpolarizing and depolarizing actions of dopamine via D-1 and D-2 receptors on nucleus accumbens neurons. *Brain Res* 375: 368–372, 1986.

Uchimura N, North RA. Actions of cocaine on rat nucleus accumbens neurones in vitro. *Br J Pharmacol* 99: 736–740, 1990.

Umemiya M, Raymond LA. Dopaminergic modulation of excitatory postsynaptic currents in rat neostriatal neurons. *J Neurophysiol* 78: 1248–1255, 1997.

Vallone D, Picetti R, Borrelli E. Structure and function of dopamine receptors. *Neurosci Biobehav Rev* 24: 125–132, 2000.

Vergara R, Rick C, Hernández-Lóopez S, Laville JA, Guzman JN, Galarraga E, Surmeier DJ, Bargas J. Spontaneous voltage oscillations in striatal projection neurons in a rat corticostriatal slice. *J Physiol* 553: 169–182, 2003.

Vilchis C, Bargas J, Ayala GX, Galvan E, Galarraga E. Ca^{2+} channels that activate Ca^{2+}-dependent K^+ currents in neostriatal neurons. *Neuroscience* 95: 745–752, 2000.

White FJ, Hu XT, Zhang XF. DA D2 receptors in the ventral striatum: multiple effects or receptor subtypes? *Nihon Shinkei Seishin Yakurigaku Zasshi* 17: 91–95, 1997.

Wickens JR, Wilson CJ. Regulation of action-potential firing in spiny neurons of the rat neostriatum in vivo. *J Neurophysiol* 79: 2358–2364, 1998.

Wilson CJ. Dendritic morphology, inward rectification, and the functional properties of neostriatal neurons. In: *Single Neuron Computation*, edited by McKenna T, Davis J, Zornetzer S. New York: Academic Press, 1992, p. 141–171.

Wilson CJ, Kawaguchi Y. The origins of two-state spontaneous membrane potential fluctuations of neostriatal spiny neurons. *J Neurosci* 16: 2397–2410, 1996.

Wolf JA, Eleey C, Finkel LH, Contreras D. Sublinear summation of inputs in the nucleus accumbens of the awake rat. Program No. 517.10. *2005 Abstract Viewer and Itinerary Planner*. Washington, DC: Society for Neuroscience, 2005a, Online.

Wolf JA, Moyer JT, Lazarewicz MT, Contreras D, Benoit-Marand M, O'Donnell P, Finkel LH. NMDA/AMPA ratio impacts state transitions and entrainment to oscillations in a computational model of the nucleus accumbens medium spiny projection neuron. *J Neurosci* 25: 9080–9095, 2005b.

Yasuda R, Sabatini BL, Svoboda K. Plasticity of calcium channels in dendritic spines. *Nat Neurosci* 6: 948–955, 2003.

Yim CY, Mogenson GJ. Neuromodulatory action of dopamine in the nucleus accumbens: an in vivo intracellular study. *Neuroscience* 26: 403–415, 1988.

Yung KK, Bolam JP, Smith AD, Hersch SM, Ciliax BJ, Levey AI. Immunocytochemical localization of D1 and D2 dopamine receptors in the basal ganglia of the rat: light and electron microscopy. *Neuroscience* 65: 709–730, 1995.

Zhang XF, Cooper DC, White FJ. Repeated cocaine treatment decreases whole-cell calcium current in rat nucleus accumbens neurons. *J Pharmacol Exp Ther* 301: 1119–1125, 2002.

Zhang XF, Hu XT, White FJ. Whole-cell plasticity in cocaine withdrawal: reduced sodium currents in nucleus accumbens neurons. *J Neurosci* 18: 488–498, 1998.